QC
807.5
U603
no.13

NOAA Technical Memorandum ERL OD-13

U.S. DEPARTMENT OF COMMERCE
NATIONAL OCEANIC AND ATMOSPHERIC ADMINISTRATION
Environmental Research Laboratories

Comparison of a Hydrostatic and an Anelastic Dry Shallow Primitive Equation Model

ROGER PIELKE

Office
of the Director
BOULDER,
COLORADO
February 1972

RONMENTAL RESEARCH LABORATORIES

OFFICE OF THE DIRECTOR

IMPORTANT NOTICE

Technical Memoranda are used to insure prompt dissemination of special studies which, though of interest to the scientific community, may not be ready for formal publication. Since these papers may later be published in a modified form to include more recent information or research results, abstracting, citing, or reproducing this paper in the open literature is not encouraged. Contact the author for additional information on the subject matter discussed in this Memorandum.

NATIONAL OCEANIC AND ATMOSPHERIC ADMINISTRATION

BOULDER, COLORADO

QC
807.5
.U6O3
no.13

U.S. DEPARTMENT OF COMMERCE
National Oceanic and Atmospheric Administration
Environmental Research Laboratories

NOAA Technical Memorandum ERL OD-13

COMPARISON OF A HYDROSTATIC AND AN ANELASTIC DRY SHALLOW PRIMITIVE EQUATION MODEL

Roger Pielke

Experimental Meteorology Laboratory

ATMOSPHERIC SCIENCES
LIBRARY
JUL 17 1972
N.O.A.A.
U. S. Dept. of Commerce

Office of the Director
Boulder, Colorado
February 1972

'72 3475

ATMOSPHERIC SCIENCES
LIBRARY
JUL 17 1972
N.O.A.A.
U. S. Dept. of Commerce

TABLE OF CONTENTS

ABSTRACT

The adequacy of the hydrostatic assumption in mesoscale-subsynoptic models is examined for various horizontal grid intervals, heat inputs and thermal stabilities. To accomplish this, a hydrostatic and an anelastic two dimensional, dry, shallow primitive equation model are developed coincidentally and compared for the same initial and boundary conditions. A simplified technique to compute the pressure in the anelastic model is introduced.

The models have 13 vertical and 21 horizontal grid points. Heat is introduced into the models over seven horizontal grid points at the bottom two levels. The vertical grid interval is fixed and the horizontal grid interval varied. A sinusoidal heating function is prescribed. The large scale advective velocity is 1 m/sec.

The study, while not exhaustive, suggests that the hydrostatic assumption may be adequate, particularly for dry models, with horizontal grid intervals as small as 1 km. Smaller heat inputs and more stable thermal stratifications improve the accuracy of the hydrostatic assumption for a given horizontal grid interval. The horizontal grid interval is more important than the magnitude of vertical motion in determining the adequacy of the hydrostatic assumption.

For vertical and horizontal grid intervals of 300m, the convergence zones have a larger amplitude and the upwind convergence zone propagates downstream more rapidly in the hydrostatic model than in the anelastic model. The effect of the nonhydrostatic pressure is to create a relative low pressure aloft and relative high pressure below. The nonhydrostatic pressure gradient is then counter to the hydrostatic pressure gradient.

COMPARISON OF A HYDROSTATIC AND AN ANELASTIC DRY SHALLOW PRIMITIVE EQUATION MODEL

Roger Pielke

1. INTRODUCTION

Many mesoscale-subsynoptic models use the hydrostatic assumption to determine the pressure field. The justification is based on scale arguements similar to that given by Haltiner (1968): if

$$\frac{D^2}{L^2} << 1 \qquad (1)$$

then the hydrostatic assumption is valid where D and L are characteristic vertical and horizontal scales and correspond roughly to 1/4 wavelength of the disturbance. Hovermale (1965) obtained the same result by considering the effect of neglect of vertical accelerations on gravity wave oscillations. Estoque (1961, 1962), Moroz (1967), McPherson (1970), Delage and Taylor (1970) and Estoque and Bhumralkar (1968) justify the use of the hydrostatic assumption through scale arguements. Delage and Taylor have a horizontal grid of .5 km in some of their calculations, whereas Estoque's minimum horizontal grid is 2 km.

In contrast, Neumann and Mahyer (1971) argue that scale analysis shows the hydrostatic assumption cannot be used to model land and sea breeze scale circulations.

Indeed, scale arguements alone only define the limiting case in which a hydrostatic model can be used. It fails to describe the magnitude and significance of errors induced in a hydrostatic model if criterion (1) is not adequately fulfilled.

Laboratory results by Hide (1958), in fact, suggest that hydrostatic balance may be maintained even if D/L approaches unity provided

that geostrophic flow with a "stable enough" density stratification exists.

The purpose of this paper will be to delineate the horizontal scales for which a hydrostatic model can be used accurately. The vertical scales are limited by the stable stratification and the depth of the atmosphere.

A hydrostatic and an anelastic, dry, shallow, primitive equation model are developed coincidentally and tested with the same initial and boundary conditions. The basic hypothesis is that the hydrostatic and anelastic models will yield identical solutions when the horizontal grid interval is large compared to the vertical grid interval. As the models are refined by decreasing the horizontal grid interval, the solutions are examined to see if and by how much they diverge from one another. The heat which drives the circulation is introduced over a constant number of grid points. The effect of varying thermal stratification and different heat input is examined. A simplified technique to compute the anelastic pressure is developed.

2. EQUATIONS

The equation of motion for inviscid, non-electromagnetic fluid flow in a rotating coordinate system is (symbols are defined in the Appendix).

$$\frac{\partial U_i}{\partial t} = -U_j \frac{\partial U_i}{\partial x_j} - \frac{1}{\rho} \frac{\partial p}{\partial x_i} - g \delta_{i3} - 2\varepsilon_{ijk} \Omega_j U_k. \qquad (2)$$

If the fluid is an ideal gas, then

$$\frac{1}{\rho} \frac{\partial p}{\partial x_i} = \Theta \frac{\partial \Pi}{\partial x_i}. \qquad (3)$$

The first law of thermodynamics for an ideal gas under adiabatic

conditions is

$$\frac{\partial \Theta}{\partial t} = -U_j \frac{\partial \Theta}{\partial x_j} . \tag{4}$$

The continuity equation for incompressible flow is

$$\frac{\partial U_i}{\partial x_i} = 0. \tag{5}$$

Dutton and Fichtl (1969) have demonstrated that the continuity equation (5) is adequate to describe shallow motion or motion which occurs over a depth much less than the scale depth of the atmosphere.

In relation to the real atmosphere, the following assumptions have been incorporated into the equations:

1. molecular viscosity and conduction are neglected.
2. radiation effects are neglected.
3. moisture effects are neglected.
4. the motions to be described by the equations are confined to the lowest few kilometers.

The dependent variables A_i (i.e. U_i or Θ or Π) are decomposed into

$$A_i = \hat{A}_i + \tilde{A}_i + A'_i \text{ where} \tag{6}$$

$$\hat{A}_i = \frac{\iiint_D A_i \, dx_1 dx_2 dx_3}{\iiint_D dx_1 dx_2 dx_3} \tag{7}$$

$$\tilde{A}_i = \frac{\iiint_d (A_i - \hat{A}_i) dx_1 dx_2 dx_3}{\iiint_d dx_1 dx_2 dx_3} \tag{8}$$

$$A'_i = A_i - (\hat{A}_i + \tilde{A}_i) . \tag{9}$$

and $\hat{A}_i$ is an average value of A_i over the entire model domain D. The variable $\tilde{A}_i$ is the deviation of A_i from $\hat{A}_i$ averaged over a grid domain d.

An averaging operator is defined by

$$\overline{A}_i = \frac{\iiint_d A_i \, dx_1 dx_2 dx_3}{\iiint_d dx_1 dx_2 dx_3} \tag{10}$$

It follows directly that

$$\overline{A'} = \overline{A_i - (\hat{A}_i + \tilde{A}_i)} \tag{11}$$

$$= \overline{(A_i - \hat{A}_i) - \tilde{A}}$$

$$= \overline{A_i - \hat{A}_i} - \overline{\tilde{A}}$$

$$= \tilde{A}_i - \tilde{A}_i$$

$$= 0.$$

The domain averaged variables of the model are assumed governed by

$$\frac{\partial \hat{U}_i}{\partial t} = -\hat{U}_j \frac{\partial \hat{U}_i}{\partial x_j} - \hat{\Theta} \frac{\partial \hat{\Pi}}{\partial x_i} - g \, \delta_{i3} - 2\varepsilon_{ijk}\Omega_j \hat{U}_k, \tag{12}$$

$$\frac{\partial \hat{\Theta}}{\partial t} = -\hat{U}_j \frac{\partial \hat{\Theta}}{\partial x_j}, \text{ and} \tag{13}$$

$$\frac{\partial \hat{U}_i}{\partial x_i} = 0. \tag{14}$$

Substituting expression (6) into (2), (4) and (5) and averaging as defined by (10) yields

$$\frac{\partial \hat{U}_i}{\partial t} + \frac{\partial \tilde{U}_i}{\partial t} = -\hat{U}_j \frac{\partial \hat{U}_j}{\partial x_j} - (\hat{U}_j + \tilde{U}_j)\frac{\partial \tilde{U}_i}{\partial x_j} - \tilde{U}_j \frac{\partial \hat{U}_i}{\partial x_j} - \overline{U_j' \frac{\partial U_i'}{\partial x_j}} \qquad (15)$$

$$- \hat{\Theta} \frac{\partial \hat{\Pi}}{\partial x_i} - (\hat{\Theta}+\tilde{\Theta})\frac{\partial \tilde{\Pi}}{\partial x_i} - \tilde{\Theta}\frac{\partial \hat{\Pi}}{\partial x_i} - \overline{\Theta' \frac{\partial \Pi'}{\partial x_i}}$$

$$-2\varepsilon_{ijk}\Omega_j \tilde{U}_k - 2\varepsilon_{ijk}\Omega_j \hat{U}_k - g\,\delta_{i3}$$

$$\frac{\partial \hat{\Theta}}{\partial t} + \frac{\partial \tilde{\Theta}}{\partial t} = -\hat{U}_j \frac{\partial \hat{\Theta}}{\partial x_j} - (\hat{U}_j + \tilde{U}_j)\frac{\partial \tilde{\Theta}}{\partial x_j} - \tilde{U}_j \frac{\partial \hat{\Theta}}{\partial x_j} - \overline{U_j' \frac{\partial \Theta'}{\partial x_j}}, \text{ and} \qquad (16)$$

$$\frac{\partial \hat{U}_i}{\partial x_i} + \frac{\partial \tilde{U}_i}{\partial x_i} = 0. \qquad (17)$$

The equations for the grid-interval averaged variables are obtained by substracting (12), (13) and (14) from (15), (16) and (17), respectively. Thus,

$$\frac{\partial \tilde{U}_i}{\partial t} = -(\hat{U}_j + \tilde{U}_j)\frac{\partial \tilde{U}_i}{\partial x_j} - \tilde{U}_j \frac{\partial \hat{U}_i}{\partial x_j} - \overline{U_j' \frac{\partial U_i'}{\partial x_j}} - (\hat{\Theta}+\tilde{\Theta})\frac{\partial \tilde{\Pi}}{\partial x_i} - \tilde{\Theta}\frac{\partial \hat{\Pi}}{\partial x_i} \qquad (18)$$

$$\overline{-\Theta' \frac{\partial \Pi'}{\partial x_i}} - 2\varepsilon_{ijk}\Omega_j \tilde{U}_k,$$

$$\frac{\partial \tilde{\Theta}}{\partial t} = -(\hat{U}_j + \tilde{U}_j)\frac{\partial \tilde{\Theta}}{\partial x_j} - \tilde{U}_j \frac{\partial \hat{\Theta}}{\partial x_j} - \overline{U_j' \frac{\partial \Theta'}{\partial x_j}}, \text{ and} \qquad (19)$$

$$\frac{\partial \tilde{U}_i}{\partial x_i} = 0. \qquad (20)$$

Equation (18) is simplified by assuming the deviation of the grid-interval averaged potential temperature from the model domain averaged potential temperature is small. The fourth term on the right of (18) reduces to

$$(\hat{\Theta}+\tilde{\Theta})\frac{\partial \tilde{\Pi}}{\partial x_i} = \hat{\Theta}\left(1+\frac{\tilde{\Theta}}{\hat{\Theta}}\right)\frac{\partial \tilde{\Pi}}{\partial x_i} \simeq \hat{\Theta}\frac{\partial \tilde{\Pi}}{\partial x_i}, \text{ for } \tilde{\Theta}/\hat{\Theta} << 1. \qquad (21)$$

Further, if the model domain-averaged pressure is assumed hydrostatic, then

$$\tilde{\Theta}\,\frac{\partial\hat{\Pi}}{\partial x_3} = \frac{-\tilde{\Theta}}{\hat{\Theta}}\,g. \tag{22}$$

With these assumptions, (18) reduces to

$$\frac{\partial\tilde{U}_i}{\partial t} = -(\hat{U}_j+\tilde{U}_j)\frac{\partial\tilde{U}_i}{\partial x_j} - \tilde{U}_j\,\frac{\partial\hat{U}_i}{\partial x_j} - \hat{\Theta}\frac{\partial\tilde{\Pi}}{\partial x_i} - (1-\delta_{i3})\tilde{\Theta}\frac{\partial\hat{\Pi}}{\partial x_i} \tag{23}$$

$$-2\varepsilon_{ijk}\Omega_j\tilde{U}_k + \frac{\tilde{\Theta}}{\hat{\theta}}\,g - \left(\overline{U'_j\frac{\partial U'_i}{\partial x_j}} + \overline{\Theta\frac{\partial\Pi'}{\partial x_i}}\right).$$

This system of equations (19), (20) and (23) involves the dependent variables $\tilde{U}_i$, $\tilde{\Theta}$ and $\tilde{\Pi}$ as a function of x_i and t. The equations, however, cannot be closed without knowledge of the last term on the right of (23). Typically, the second part of this term is neglected because pressure has little energy at high wave numbers (Lumley and Panofsky, 1966). The first part of the term, (the Reynolds stress), is approximated in analogy to molecular viscosity, by an eddy viscosity formulation.

$$\overline{U'_iU'_j} \simeq -K_{ij}^{(m)}\,\frac{\partial(\tilde{U}_i+\hat{U}_i)}{\partial x_j} \tag{24}$$

Although such an eddy coefficient formulation is, at best, first order turbulence theory, it has been used satisfactorily in many mesoscale-subsynoptic models. The eddy coefficient is either assumed constant or a function of the grid domain averaged variable.

Similarly, the Reynolds flux term in (19) is estimated.

by

$$\overline{U_j'\Theta'} \simeq -K_j^{(\Theta)}\,\frac{\partial(\tilde{\Theta}+\hat{\Theta})}{\partial x_j}\,. \tag{25}$$

3. HYDROSTATIC MODEL

If the vertical acceleration and Reynold stress terms are neglected relative to the vertical pressure gradient and gravitational acceleration terms in (23), the pressure can then be computed from

$$\frac{\partial \tilde{\Pi}_H}{\partial z} = \frac{\tilde{\Theta}}{\hat{\Theta}^2} g \tag{26}$$

The remaining equations are given by

$$\frac{\partial \tilde{U}_1}{\partial t} = -(\hat{U}_j+\tilde{U}_j)\frac{\partial \tilde{U}_1}{\partial x_j} - \tilde{U}_j\frac{\partial \hat{U}_1}{\partial x_j} - \hat{\Theta}\frac{\partial \tilde{\Pi}_H}{\partial x_1} - \tilde{\Theta}\frac{\partial \hat{\Pi}}{\partial x_1} - 2\varepsilon_{1jk}\Omega_j\tilde{U}_k \tag{27}$$

$$+ \frac{\partial}{\partial x_j}\left[K_{1j}^{(m)}\frac{\partial(\tilde{U}_1+\hat{U}_1)}{\partial x_j}\right], \qquad (1 = 1,2)$$

$$\frac{\partial \tilde{\Theta}}{\partial t} = -(\hat{U}_j+\tilde{U}_j)\frac{\partial \tilde{\Theta}}{\partial x_j} - \tilde{U}_j\frac{\partial \hat{\Theta}}{\partial x_j} + \frac{\partial}{\partial x_j}\left[K_j^{(\Theta)}\frac{\partial(\tilde{\Theta}+\hat{\Theta})}{\partial x_j}\right], \tag{28}$$

and

$$\frac{\partial \tilde{U}_i}{\partial x_i} = 0. \tag{29}$$

To simplify the problem, the following assumptions are made:

1. $\frac{\partial}{\partial x_2} = \frac{\partial}{\partial y} \equiv 0$;

2. $\frac{\partial \hat{U}_1}{\partial x_j} \equiv 0$;

3. $\frac{\partial \hat{\Pi}}{\partial x_1} \equiv 0$;

4. $\frac{\partial \hat{\Theta}}{\partial x_1} \equiv 0$;

5. $\hat{U}_2 = \hat{V} \equiv 0; \quad \hat{U}_3 = \hat{W} \equiv 0; \quad \tilde{U}_2 = \tilde{V} \equiv 0$

6. $K_{lj}^{(m)} = K_j^{(\Theta)} \equiv 0;$

and

7. $\Omega_j \equiv 0.$ $\qquad \begin{pmatrix} l = 1,2 \\ j = 1,2,3 \\ i = 1,2,3 \end{pmatrix}$

Equations (26), (27), (28) and (29) in component form then reduce to

$$\frac{\partial \tilde{\Pi}_H}{\partial z} = \frac{\tilde{\Theta}}{\hat{\Theta}^2} g, \tag{30}$$

$$\frac{\partial \tilde{U}}{\partial t} = -(\hat{U}+\tilde{U})\frac{\partial \tilde{U}}{\partial x} - \tilde{W}\frac{\partial \tilde{U}}{\partial z} - \hat{\Theta}\frac{\partial \tilde{\Pi}_H}{\partial x}, \tag{31}$$

$$\frac{\partial \tilde{\Theta}}{\partial t} = -(\hat{U}+\tilde{U})\frac{\partial \tilde{\Theta}}{\partial x} - \tilde{W}\left(\frac{\partial \tilde{\Theta}}{\partial z} + \frac{\partial \hat{\Theta}}{\partial z}\right), \tag{32}$$

and

$$\frac{\partial \tilde{W}}{\partial z} = -\frac{\partial \tilde{U}}{\partial x} \tag{33}$$

The boundary conditions are

$$\tilde{\Pi}_H = \tilde{U} = \tilde{W} = \tilde{\Theta} = 0. \qquad \text{lateral} \tag{34}$$

$$\tilde{\Pi}_H = \tilde{U} = \tilde{\Theta} = 0 \qquad \text{top}$$

$$\left.\begin{aligned} &\tilde{U} = \tilde{W} = 0 \\ &\tilde{\Theta} = A(x) \sin \frac{3.14159t}{T} \end{aligned}\right\} \qquad \text{bottom}$$

At the initial time

$$\tilde{U} = \tilde{W} = \tilde{\Theta} = \tilde{\Pi}_H = 0. \tag{35}$$

The hydrostatic model consists of two prognostic equations ((31) and (32)) for $\tilde{U}$ and $\tilde{\Theta}$ and two diagnostic equations, ((30) and (33)) for $\tilde{\Pi}_H$ and $\tilde{W}$.

4. ANELASTIC MODEL

When the magnitude of the vertical acceleration is comparable to the pressure gradient and gravitational acceleration terms in (23), an equation for pressure can be obtained by taking the three dimensional divergence of (23) and solving for the Laplacian of pressure:

$$\frac{\partial^2 \tilde{\Pi}_A}{\partial x_i^2} = -\frac{1}{\hat{\Theta}}\frac{\partial}{\partial t}\cancel{\frac{\partial \tilde{U}_i}{\partial x_i}} + \frac{1}{\hat{\Theta}^2}\frac{\partial \tilde{U}_i}{\partial t}\frac{\partial \hat{\Theta}}{\partial x_i} - \frac{\partial}{\partial x_i}\frac{(\hat{U}_j+\tilde{U}_j)}{\hat{\Theta}}\frac{\partial \tilde{U}_i}{\partial x_j} \qquad (36)$$

$$- \frac{\partial}{\partial x_i}\frac{\tilde{U}_j}{\hat{\Theta}}\frac{\partial \hat{U}_i}{\partial x_j} - (1-\delta_{i3})\frac{\partial}{\partial x_i}\frac{\tilde{\Theta}}{\hat{\Theta}}\frac{\partial \hat{\Pi}}{\partial x_i} + g\delta_{i3}\frac{\partial}{\partial x_i}\frac{\tilde{\Theta}}{\hat{\Theta}^2}$$

$$- 2\varepsilon_{ijk}\frac{\partial}{\partial x_i}\Omega_j\frac{\tilde{U}_k}{\hat{\Theta}} + \frac{\partial}{\partial x_i}\frac{1}{\hat{\Theta}}\frac{\partial}{\partial x_j}\Big\langle^{(m)}_{ij}\frac{\partial(\tilde{U}_i+\hat{U}_i)}{\partial x_j}.$$

The first term on the right side of (36) is identically zero by virtue of the continuity equation (20). (36) is of the form Ogura and Charney (1961), Neumann and Mahyer (1971) and Brundidge, et al. (1971) used to compute the pressure. However, pressure can be obtained by a somewhat simpler approach.

The Laplacian of the hydrostatic pressure is obtained by the addition of the horizontal divergence of the horizontal component of the equation of motion (23) and the derivative of the hydrostatic relation (26) with respect to height. Thus,

$$\frac{\partial^2 \Pi_H}{\partial x_i^2} = -\frac{1}{\hat{\Theta}}\frac{\partial}{\partial x_1}\frac{\partial \overset{*}{\tilde{U}}_1}{\partial t} + \frac{1}{\hat{\Theta}^2}\frac{\partial \hat{\Theta}}{\partial x_1}\frac{\partial \overset{*}{\tilde{U}}_1}{\partial t} - \frac{\partial}{\partial x_1}\frac{(\hat{U}_j+\tilde{U}_j)}{\hat{\Theta}}\frac{\partial \tilde{U}_1}{\partial x_j} \qquad (37)$$

$$- \frac{\partial}{\partial x_1}\frac{\tilde{U}_j}{\hat{\Theta}}\frac{\partial \hat{U}_1}{\partial x_j} - (1-\delta_{i3})\frac{\partial}{\partial x_1}\frac{\tilde{\Theta}}{\hat{\Theta}}\frac{\partial \hat{\Pi}}{\partial x_1} - 2\varepsilon_{1jk}\frac{\partial}{\partial x_1}\Omega_j\frac{\tilde{U}_k}{\hat{\Theta}}$$

$$+ \frac{\partial}{\partial x_1}\frac{1}{\hat{\Theta}}\frac{\partial}{\partial x_j}\Big\langle^{(m)}_{1j}\frac{\partial}{\partial x_j}(\tilde{U}_1+\hat{U}_1) + g\delta_{i3}\frac{\partial}{\partial x_i}\frac{\tilde{\Theta}}{\hat{\Theta}^2}$$

$$(1 = 1,2;\ i = 1,2,3),$$

where $\overset{*}{\tilde{U}}_1$ is a hydrostatic velocity forced by a hydrostatic pressure gradient.

Subtracting (37) from (36) yields

$$\frac{\partial^2 R}{\partial x_i^2} = \frac{\partial^2}{\partial x_i^2}(\tilde{\Pi}_A - \tilde{\Pi}_H) = + \frac{1}{\hat{\Theta}} \frac{\partial}{\partial x_1} \frac{\partial \overset{*}{\tilde{U}}_1}{\partial t} \tag{38}$$

$$+ \frac{1}{\hat{\Theta}^2} \left[\frac{\partial \tilde{U}_i}{\partial t} \frac{\partial \hat{\Theta}}{\partial x_i} - \frac{\partial \overset{*}{\tilde{U}}_1}{\partial t} \frac{\partial \hat{\Theta}}{\partial x_1} \right] - \left[\frac{\partial}{\partial x_i} \frac{(\tilde{U}_j + \hat{U}_j)}{\hat{\Theta}} \frac{\partial \tilde{U}_i}{\partial x_j} - \frac{\partial}{\partial x_1} \frac{(\tilde{U}_j + \hat{U}_j)}{\hat{\Theta}} \frac{\partial \tilde{U}_1}{\partial x_j} \right]$$

$$- \left[\frac{\partial}{\partial x_i} \frac{\tilde{U}_j}{\hat{\Theta}} \frac{\partial \hat{U}_i}{\partial x_j} - \frac{\partial}{\partial x_1} \frac{\tilde{U}_j}{\hat{\Theta}} \frac{\partial \hat{U}_1}{\partial x_j} \right] - (1 - \delta_{i3}) \left[\frac{\partial}{\partial x_i} \frac{\tilde{\Theta}}{\hat{\Theta}} \frac{\partial \hat{\Pi}}{\partial x_i} - \frac{\partial}{\partial x_1} \frac{\tilde{\Theta}}{\hat{\Theta}} \frac{\partial \hat{\Pi}}{\partial x_1} \right]$$

$$+ g\delta_{i3} \left(\frac{\partial}{\partial x_i} \frac{\tilde{\Theta}}{\hat{\Theta}^2} - \frac{\partial}{\partial x_i} \frac{\tilde{\Theta}}{\hat{\Theta}^2} \right) - 2 \left[\varepsilon_{ijk} \frac{\partial}{\partial x_i} \Omega_j \frac{\tilde{U}_k}{\hat{\Theta}} - \varepsilon_{1jk} \frac{\partial}{\partial x_1} \Omega_j \frac{\tilde{U}_k}{\hat{\Theta}} \right]$$

$$+ \left[\frac{\partial}{\partial x_i} \frac{1}{\hat{\Theta}} \frac{\partial}{\partial x_j} \Big\langle^{(m)}_{ij} \frac{\partial U_i}{\partial x_j} - \frac{\partial}{\partial x_1} \frac{1}{\hat{\Theta}} \frac{\partial}{\partial x_j} \Big\langle^{(m)}_{1j} \frac{\partial U_1}{\partial x_j} \right]$$

$$\left(\begin{matrix} 1 = 1,2 \\ i = 1,2,3 \end{matrix} \right),$$

which reduces to

$$\frac{\partial^2 R}{\partial x_i^2} = \frac{1}{\hat{\Theta}} \frac{\partial}{\partial x_1} \frac{\partial \overset{*}{\tilde{U}}}{\partial t} + \frac{1}{\hat{\Theta}^2} \left[\frac{\partial \tilde{U}_i}{\partial t} \frac{\partial \hat{\Theta}}{\partial x_i} - \frac{\partial \overset{*}{\tilde{U}}_1}{\partial t} \frac{\partial \hat{\Theta}}{\partial x_1} \right] \tag{39}$$

$$- \frac{\partial}{\partial x_i} \frac{(\tilde{U}_j + \hat{U}_j)}{\hat{\Theta}} \frac{\partial \tilde{U}_i}{\partial x_j} \delta_{i3} - \frac{\partial}{\partial x_i} \frac{\tilde{U}_j}{\hat{\Theta}} \frac{\partial \hat{U}_i}{\partial x_j} \delta_{i3}$$

$$- 2\varepsilon_{ijk} \frac{\partial}{\partial x_i} \Omega_j \frac{\tilde{U}_k}{\hat{\Theta}} \delta_{i3} + \frac{\partial}{\partial x_i} \frac{1}{\hat{\Theta}} \frac{\partial}{\partial x_j} \Big\langle^{(m)}_{ij} \frac{\partial U_i}{\partial x_j} \delta_{i3}$$

$$\left(\begin{matrix} 1 = 1,2 \\ i = 1,2,3 \end{matrix} \right).$$

The total anelastic pressure is obtained by integrating (26) for $\tilde{\Pi}_H$ and solving the elliptic differential equation (39) for R and adding

$$\tilde{\Pi}_A = \tilde{\Pi}_H + R \,. \tag{40}$$

The remaining equations are given by

$$\frac{\partial \tilde{U}_l}{\partial t} = -(\tilde{U}_j+\hat{U}_j)\frac{\partial \tilde{U}_l}{\partial x_j} - \tilde{U}_j\frac{\partial \hat{U}_l}{\partial x_j} - \hat{\Theta}\frac{\partial \tilde{\Pi}_A}{\partial x_l} - \tilde{\Theta}\frac{\partial \hat{\Pi}}{\partial x_l} - 2\varepsilon_{ljk}\Omega_j\tilde{U}_k \quad (41)$$

$$+ \frac{\partial}{\partial x_j}\underline{K}^{(m)}_{lj}\frac{\partial}{\partial x_j}(\tilde{\underline{U}}_l+\hat{\underline{U}}_l) \ ,$$

$$\frac{\partial \tilde{\Theta}}{\partial t} = -(\hat{U}_j+\tilde{U}_j)\frac{\partial \tilde{\Theta}}{\partial x_j} - \tilde{U}_j\frac{\partial \hat{\Theta}}{\partial x_j} + \frac{\partial}{\partial x_j}K^{(\Theta)}_j\frac{\partial}{\partial x_j}(\tilde{\Theta}+\hat{\Theta}) \ , \quad (42)$$

$$\frac{\partial \tilde{U}_i}{\partial x_i} = 0 \ , \text{ and} \quad (43)$$

$$\frac{\partial \overset{*}{\tilde{U}}_l}{\partial t} = -(\tilde{U}_j+\hat{U}_j)\frac{\partial \tilde{U}_l}{\partial x_j} - \tilde{U}_j\frac{\partial \hat{U}_l}{\partial x_j} - \hat{\Theta}\frac{\partial \tilde{\Pi}_H}{\partial x_l} - \tilde{\Theta}\frac{\partial \hat{\Pi}}{\partial x_l} - 2\varepsilon_{ljk}\Omega_j\tilde{U}_k \quad (44)$$

$$+ \frac{\partial}{\partial x_j}\underline{K}^{(m)}_{lj}\frac{\partial}{\partial x_j}(\tilde{\underline{U}}_l+\hat{\underline{U}}_l) \ .$$

The following assumptions, consistent with the hydrostatic model given in section 3, are made:

1. $\frac{\partial}{\partial x_2} = \frac{\partial}{\partial y} = 0;$

2. $\frac{\partial \hat{U}_l}{\partial x_j} \equiv 0;$

3. $\frac{\partial \hat{\Pi}}{\partial x_l} \equiv 0;$

4. $\frac{\partial \hat{\Theta}}{\partial x_l} \equiv 0;$

5. $\hat{U}_2 = \hat{V} \equiv 0; \quad \hat{U}_3 = \hat{W} \equiv 0; \tilde{U}_2 = \tilde{V} \equiv 0$

6. $\underline{K}^{(m)}_{ij} = K^{(\Theta)}_j \equiv 0;$

7. $\Omega_j \equiv 0.$

$\left(\begin{matrix} j = 1,2,3 \\ i = 1,2,3 \\ l = 1,2 \end{matrix}\right)$

Equations (39), (40), (26), (41), (42), (43), and (44)

reduce to

$$\frac{\partial \tilde{\Pi}_H}{\partial z} = \frac{\tilde{\Theta}}{\hat{\Theta}^2} g, \tag{45}$$

$$\nabla^2 R = \frac{1}{\hat{\Theta}} \frac{\partial}{\partial x} \overset{*}{\frac{\partial \tilde{U}}{\partial t}} + \frac{1}{\hat{\Theta}^2} \frac{\partial \tilde{W}}{\partial t} \frac{\partial \hat{\Theta}}{\partial z} - \frac{\partial}{\partial z} \frac{(\tilde{U}+\hat{U})}{\hat{\Theta}} \frac{\partial \tilde{W}}{\partial x} - \frac{\partial}{\partial z} \frac{\tilde{W}}{\hat{\Theta}} \frac{\partial \tilde{W}}{\partial z}, \tag{46}$$

$$\tilde{\Pi}_A = \tilde{\Pi}_H + R, \tag{47}$$

$$\frac{\partial \tilde{U}}{\partial t} = -(\tilde{U}+\hat{U}) \frac{\partial \tilde{U}}{\partial x} - \tilde{W} \frac{\partial \tilde{U}}{\partial z} - \hat{\Theta} \frac{\partial \tilde{\Pi}_A}{\partial x}, \tag{48}$$

$$\frac{\partial \tilde{\Theta}}{\partial t} = -(\tilde{U}+\hat{U}) \frac{\partial \tilde{\Theta}}{\partial x} - \tilde{W} \left[\frac{\partial \tilde{\Theta}}{\partial z} + \frac{\partial \hat{\Theta}}{\partial z} \right], \tag{49}$$

$$\frac{\partial \tilde{W}}{\partial z} = -\frac{\partial \tilde{U}}{\partial x}, \tag{50}$$

and

$$\overset{*}{\frac{\partial \tilde{U}}{\partial t}} = -(\tilde{U}+\hat{U}) \frac{\partial \tilde{U}}{\partial x} - \tilde{W} \frac{\partial \tilde{U}}{\partial z} - \hat{\Theta} \frac{\partial \tilde{\Pi}_H}{\partial x}. \tag{51}$$

The boundary conditions are

$$R = \tilde{\Pi}_H = \tilde{\Pi}_A = \tilde{U} = \tilde{W} = \tilde{\Theta} = 0 \quad \text{lateral}, \tag{52}$$

$$R = \tilde{\Pi}_H = \tilde{\Pi}_A = \tilde{U} = \tilde{\Theta} = 0 \quad \text{top},$$

$$\tilde{U} = \tilde{W} = 0; \ \tilde{\Theta} = A(x) \sin \frac{3.14159t}{T}; \ \frac{\partial R}{\partial z} = 0 \quad \text{bottom}.$$

At the initial time

$$R = \tilde{U} = \tilde{W} = \tilde{\Theta} = \tilde{\Pi}_H = 0. \tag{53}$$

The anelastic model consists of three prognostic equations ((48), (49) and (51)) for $\tilde{U}$, $\tilde{\Theta}$ and $\overset{*}{\tilde{U}}$ and three diagnostic equations ((45), (46) and (50)) for $\tilde{\Pi}_H$, R and $\tilde{W}$.

With the assumptions given in this section (36) reduces to

$$\nabla^2\tilde{\Pi}_A = \frac{1}{\hat{\Theta}^2}\frac{\partial\tilde{W}}{\partial t}\frac{\partial\hat{\Theta}}{\partial z} - \frac{\partial}{\partial x}\frac{(\tilde{U}+\hat{U})}{\hat{\Theta}}\frac{\partial\tilde{U}}{\partial x} - \frac{\partial}{\partial z}(\tilde{U}+\hat{U})\frac{\partial\tilde{W}}{\partial x} - \frac{\partial}{\partial x}\frac{\tilde{W}}{\hat{\Theta}}\frac{\partial\tilde{U}}{\partial x} \quad (54)$$

$$- \frac{\partial}{\partial z}\frac{\tilde{W}}{\hat{\Theta}}\frac{\partial\tilde{W}}{\partial z} + g\frac{\partial}{\partial z}\frac{\tilde{\Theta}}{\hat{\Theta}^2} .$$

Model calculations in which (54) is used to evaluate the total pressure will be compared with identical runs in which (45) and (46) are used to calculate the total pressure.

5. NUMERICAL SCHEME

The prognostic differential equations in both models will be approximated by a semi-implicit forward upstream differencing scheme. In this scheme time derivatives are extrapolated forward in time, while advective terms are differenced one spatial grid point upstream and advected by the wind at the point. The remainder of the terms in both models will be approximated by a centered difference scheme.

Molenkamp (1968) has been very critical of forward-upstream differencing. He claims the pseudo-diffusive effect of the difference scheme is almost as large as the explicit eddy diffusion for small scale atmospheric circulations. He concludes that turbulent diffusion cannot be accurately modeled using this scheme.

Rosenthal (1969) disagrees with this conclusion. He claims many realistic results (i.e., Ogura, 1963 and Orville, 1964) have been obtained using this difference scheme. Indeed Rosenthal quotes Richtymer (1962) as finding computational damping desirable in controlling nonlinear computational instabilities.

As shown by Molenkamp, the difference equations for the prognostic variables can be written as a differential equation by expanding the prognostic variable in a second order power series in Δt and Δx. The resulting approximate expression for the computational pseudo-viscosity is

$$\nu_i = \frac{1}{2}|U_i| \left(1 - \left|\frac{U_i \Delta t}{\Delta x_i}\right|\right) \Delta x_i \ . \tag{55}$$

The implicit numerical diffusion is quite useful as a sink of energy in the two models without specifying an explicit numerical diffusion. This simplifies the finite difference form of the equations. In fact, a source of difference between the two models caused solely by finite difference techniques is eliminated. No third order derivatives appear in the elliptic differential equation for R.

The variables $\tilde{U}$, $\tilde{W}$, $\tilde{\Pi}_A$, $\tilde{\Pi}_H$ and R are defined at the same grid point. $\tilde{\Theta}$ is defined midway between the vertical grid points of the other variables. The grid is sketched in figure 1. At the top the variables are defined to be coincident.

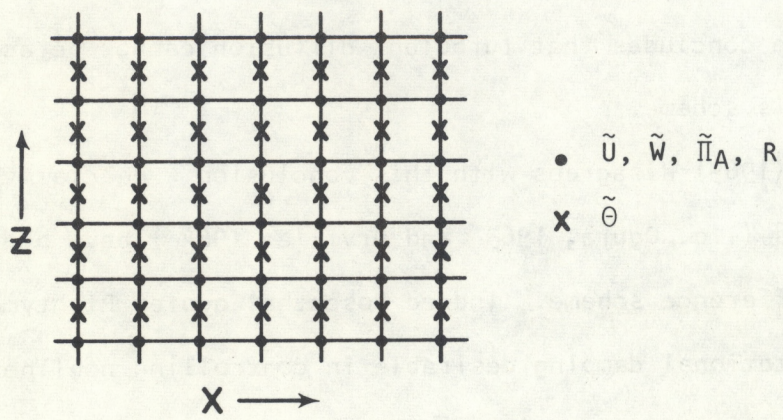

Figure 1.

The finite difference form and order of calculation of the equations in the hydrostatic model are

$$\tilde{U}^{\tau+1} = \tilde{U} - \Delta t \left[(\hat{U}+\tilde{U}) \frac{\tilde{U}-\tilde{U}_{i-1}}{x(i)-x(i-1)} + \tilde{W} \frac{\tilde{U}-\tilde{U}_{j-1}}{z(j)-z(j-1)} \right. \tag{56}$$

$$\left. \hat{\Theta} \frac{\tilde{\Pi}_H)_{i+1} - \tilde{\Pi}_H)_{i-1}}{x(i+1)-x(i-1)} \right] \text{(from (31))}.$$

$$\tilde{W}^{\tau+1} = \tilde{W}^{\tau+1}_{j-1} - \frac{\overline{\tilde{U}^{\tau+1}}^{j}_{i+1} - \overline{\tilde{U}^{\tau+1}}^{j}_{i-1}}{x(i+1)-x(i-1)} \left(z(j)-z(j-1) \right), \tag{57}$$

where

$$\overline{\tilde{U}^{\tau+1}}^{j} = (\tilde{U}^{\tau+1}_{j} + \tilde{U}^{\tau+1}_{j-1})/2 \quad \text{(from (33))}.$$

$$\tilde{\Theta}^{\tau+1} = \tilde{\Theta} - \Delta t \left[(\hat{U} + {}^{j}\overline{\tilde{U}^{\tau+1}}) \frac{\tilde{\Theta}-\tilde{\Theta}_{i-1}}{x(i)-x(i-1)} \right. \tag{58}$$

$$\left. + {}^{j}\overline{\tilde{W}^{\tau+1}} \left(\frac{\tilde{\Theta}-\tilde{\Theta}_{j-1/2}}{z(j+1/2)-z(j-1/2)} + \frac{\hat{\Theta}-\hat{\Theta}_{j-1/2}}{z(j+1/2)-z(j-1/2)} \right) \right] ,$$

where

$${}^{j}\overline{\tilde{U}^{\tau+1}} = (\tilde{U}^{\tau+1}_{j+1} + \tilde{U}^{\tau+1}_{j})/2 ,$$

$${}^{j}\overline{\tilde{W}^{\tau+1}} = (\tilde{W}^{\tau+1}_{j+1} + \tilde{W}^{\tau+1}_{j})/2 \quad \text{(from (32))},$$

and

$$\tilde{\Pi}_H{}^{\tau+1} = \tilde{\Pi}_H)^{\tau+1}_{j+1} - g \frac{\tilde{\Theta}^{\tau+1}}{\hat{\Theta}^2} \left(z(j+1)-z(j) \right) \quad \text{(from (30))}. \tag{59}$$

The finite difference form and order of calculation of the equations in the anelastic model are

$$\tilde{U}^{\tau+1} = \tilde{U} - \Delta t \left[(\hat{U}+\tilde{U}) \frac{\tilde{U}-\tilde{U}_{i-1}}{x(i)-x(i-1)} + \tilde{W} \frac{\tilde{U}-\tilde{U}_{j-1}}{z(j)-z(j-1)} \right. \tag{60}$$

$$\left. + \hat{\Theta} \frac{\tilde{\Pi}_A)_{i+1} - \tilde{\Pi}_A)_{i-1}}{x(i+1)-x(i-1)} \right] \quad \text{(from (48))}.$$

$$\left(\frac{\Delta\tilde{\overset{*}{U}}}{\Delta t}\right)^{\tau+1} = -\left[(\hat{U}+\tilde{U})\frac{\tilde{U}-\tilde{U}_{i-1}}{x(i)-x(i-1)} + \tilde{W}\frac{\tilde{U}-\tilde{U}_{j-1}}{z(j)-z(j-1)}\right. \tag{61}$$

$$\left. + \hat{\Theta}\frac{\tilde{\Pi}_H)_{i+1}-\tilde{\Pi}_H)_{i-1}}{x(i+1)-x(i-1)}\right] \qquad \text{(from (51))}.$$

$$\tilde{W}^{\tau+1} = \tilde{W}^{\tau+1}_{j-1} - \frac{\overline{\tilde{U}^{\tau+1}}^{j}_{i+1} - \overline{\tilde{U}^{\tau+1}}^{j}_{i-1}}{x(i+1)-x(i-1)}\Big(z(j)-z(j-1)\Big), \tag{62}$$

where

$$\overline{\tilde{U}^{\tau+1}}^{j} = (\tilde{U}^{\tau+1}_{j} + \tilde{U}^{\tau+1}_{j-1})/2 \quad \text{(from (50))}.$$

$$\tilde{\Theta}^{\tau+1} = \tilde{\Theta} - \Delta t\left[\left(\hat{U} + \overline{\tilde{U}^{\tau+1}}^{j}\right)\frac{\tilde{\Theta}-\tilde{\Theta}_{i-1}}{x(i)-x(i-1)}\right. \tag{63}$$

$$\left. + \overline{\tilde{W}^{\tau+1}}^{j}\left(\frac{\tilde{\Theta}-\tilde{\Theta}_{j-1/2}}{z(j+1/2)-z(j-1/2)} + \frac{\hat{\Theta}-\hat{\Theta}_{j-1/2}}{z(j+1/2)-z(j-1/2)}\right)\right],$$

where

$$\overline{\tilde{U}^{\tau+1}}^{j} = (\tilde{U}^{\tau+1}_{j+1} + \tilde{U}^{\tau+1}_{j})/2$$

$$\overline{\tilde{W}^{\tau+1}}^{j} = (\tilde{W}^{\tau+1}_{j+1} + \tilde{W}^{\tau+1}_{j})/2 \quad \text{(from (49))}.$$

The finite difference form of the Laplacian for R for variable grid intervals will be given later in this section. The forcing function of (46) is approximated by

$$\nabla^2 R^{\tau+1} \simeq \frac{1}{\overline{\hat{\Theta}}^{j}}\frac{\left(\frac{\Delta\tilde{\overset{*}{U}}}{\Delta t}\right)^{\tau+1}_{i+1} - \left(\frac{\Delta\tilde{\overset{*}{U}}}{\Delta t}\right)^{\tau+1}_{i-1}}{x(i+1)-x(i-1)} \tag{64}$$

$$+ \frac{1}{\overline{\hat{\Theta}}^{j^2}}\frac{\hat{\Theta}-\hat{\Theta}_{j-1/2}}{z(j+1/2)-z(j-1/2)}\frac{\tilde{W}^{\tau+1}-W^{\tau}}{\Delta t}$$

$$- \frac{1}{z(j+1)-z(j-1)}\left[\frac{\left(\hat{U} + \tilde{U}^{\tau+1}_{j+1}\right)}{\overline{\Theta}^{j+1}}\left(\frac{\tilde{W}^{\tau+1}_{i+1,j+1}-\tilde{W}^{\tau+1}_{i,j+1}}{x(i+1)-x(i)}\right)\right.$$

((64) continued, next page)

((64) continued)

$$- \frac{(\tilde{U}_{j-1}^{\tau+1} + \hat{U})}{\bar{\hat{\Theta}}^{j-1}} \left(\frac{\tilde{W}_{i+1,j-1}^{\tau+1} - \tilde{W}_{i,j-1}^{\tau+1}}{x(i+1)-x(i)} \right) \Bigg]$$

$$- \frac{1}{z(j+1)-z(j-1)} \left[\frac{\tilde{W}_{j+1}^{\tau+1}}{\bar{\hat{\Theta}}^{j+1}} \left(\frac{\tilde{W}_{j+2}^{\tau+1} - \tilde{W}_{j+1}^{\tau+1}}{z(j+2)-z(j+1)} \right) - \frac{\tilde{W}_{j-1}^{\tau+1}}{\bar{\hat{\Theta}}^{j-1}} \left(\frac{\tilde{W}_{j}^{\tau+1} - \tilde{W}_{j-1}^{\tau+1}}{z(j)-z(j-1)} \right) \right],$$

where

$$\bar{\hat{\Theta}}^{j} = (\Theta_{j+1/2} + \Theta_{j-1/2})/2 \ , \ \text{(from (46))},$$

$$\tilde{\Pi}_H^{\tau+1} = \tilde{\Pi}_H \Big)_{j+1}^{\tau+1} - g \frac{\tilde{\Theta}^{\tau+1}}{\hat{\Theta}^2} \Big(z(j+1)-z(j) \Big), \text{(from (45))}, \tag{65}$$

and

$$\tilde{\Pi}_A^{\tau+1} = \tilde{\Pi}_H^{\tau+1} + R^{\tau+1} \ . \quad \text{(from 47))}. \tag{66}$$

The finite difference approximation of (54) is

$$\nabla^2 \tilde{\Pi}_A^{\tau+1} \simeq \frac{1}{\bar{\hat{\Theta}}^{j^2}} \frac{\hat{\Theta}-\hat{\Theta}_{j-1/2}}{z(j+1/2)-z(j-1/2)} \frac{\tilde{W}^{\tau+1}-\tilde{W}}{\Delta t} \tag{67}$$

$$- \frac{1}{z(j+1)-z(j-1)} \left[\frac{(\tilde{U}_{j+1}^{\tau+1} + \hat{U})}{\bar{\hat{\Theta}}^{j+1}} \left(\frac{\tilde{W}_{i+1,j+1}^{\tau+1} - \tilde{W}_{i,j+1}^{\tau+1}}{x(i+1)-x(i)} \right) \right.$$

$$\left. - \frac{(\tilde{U}_{j-1}^{\tau+1} + \hat{U})}{\bar{\hat{\Theta}}^{j-1}} \left(\frac{\tilde{W}_{i+1,j-1}^{\tau+1} - \tilde{W}_{i,j-1}^{\tau+1}}{x(i+1)-x(i)} \right) \right]$$

$$- \frac{1}{z(j+1)-z(j-1)} \left[\frac{\tilde{W}_{j+1}^{\tau+1}}{\bar{\hat{\Theta}}^{j+1}} \left(\frac{\tilde{W}_{j+2}^{\tau+1} - \tilde{W}_{j+1}^{\tau+1}}{z(j+2)-z(j+1)} \right) \right.$$

$$\left. \frac{\tilde{W}_{j-1}^{\tau+1}}{\bar{\hat{\Theta}}^{j-1}} \left(\frac{\tilde{W}_{j}^{\tau+1} - \tilde{W}_{j-1}^{\tau+1}}{z(j)-z(j-1)} \right) \right] - \frac{1}{\bar{\hat{\Theta}}^{j}} \frac{1}{x(i+1)-x(i-1)}$$

$$\left[(\hat{U} + \tilde{U}_{i+1}^{\tau+1}) \frac{\tilde{U}_{i+2}^{\tau+1} - \tilde{U}_{i+1}^{\tau+1}}{x(i+2)-x(i+1)} - (\hat{U} + \tilde{U}_{i-1}^{\tau+1}) \frac{\tilde{U}_{i}^{\tau+1} - \tilde{U}_{i-1}^{\tau+1}}{x(i)-x(i-1)} \right]$$

((67) continued, next page)

((67) continued)

$$-\frac{1}{\bar{\Theta}_j}\frac{1}{x(i+1)-x(i-1)}\left[\tilde{W}^{\tau+1}_{i+1}\frac{\tilde{U}^{\tau+1}_{i+1,j+1}-\tilde{U}^{\tau+1}_{i+1,j}}{z(j+1)-z(j)}-\tilde{W}^{\tau+1}_{i-1}\frac{\tilde{U}^{\tau+1}_{i-1,j+1}-\tilde{U}^{\tau+1}_{i-1,j}}{z(j+1)-z(j)}\right]$$

$$+\frac{g}{z(j+1/2)-z(j-1/2)}\left[\frac{\tilde{\Theta}^{\tau+1}_{j+1/2}}{\hat{\Theta}^2_{j+1/2}}-\frac{\tilde{\Theta}^{\tau+1}_{j-1/2}}{\hat{\Theta}^2_{j-1/2}}\right]. \quad \text{(from (54))}.$$

In order to maintain linear computational stability, the gradient being advected must always be evaluated upstream. Therefore, the advective terms in the preceding equations have been defined such that for example:

$$\text{if } \tilde{U}+\hat{U}>0$$

$$\underline{\text{evaluate gradient}} \qquad \frac{\tilde{U}-\tilde{U}_{i-1}}{x(i)-x(i-1)}\ ;$$

$$\text{if } \tilde{U}+\hat{U}<0 \tag{68}$$

$$\underline{\text{evaluate gradient}} \qquad \frac{\tilde{U}_{i+1}-\tilde{U}}{x(i+1)-x(i)}$$

The elliptic difference equations for R and $\tilde{\Pi}_A$ are differenced consistent with the difference form of the equation of motion.

The diagnostic elliptic differential equation for R and $\tilde{\Pi}_A$ cannot be solved by simple integration. The equations for R and $\tilde{\Pi}_A$ will be solved by the method of sequential relaxation as discussed by Thompson (1961).

The elliptic equations for R and $\tilde{\Pi}_A$ are of the form

$$\nabla^2 A = F(x,z,t) \tag{69}$$

where $$A=\begin{cases}\tilde{\Pi}_A\\ R\end{cases}$$

The finite difference form of $\nabla^2 A$ will be formulated for variable

grid lengths. The Laplacian of A can be approximated by

$$\nabla^2 A \simeq \frac{1}{[x(i+1/2)-x(i-1/2)]}\left[\frac{A_{i+1}-A_i}{x(i+1)-x(i)} - \frac{A_i-A_{i-1}}{x(i)-x(i-1)}\right] \tag{70}$$

$$+ \frac{1}{[z(j+1/2)-z(j-1/2)]}\left[\frac{A_{j+1}-A_j}{z(j+1)-z(j)} - \frac{A_j-A_{j-1}}{z(j)-z(j-1)}\right].$$

Reordering (70)

$$\nabla^2 A \simeq \frac{[A_{i+1}-A_i][x(i)-x(i-1)]-[A_i-A_{i-1}][x(i+1)-x(i)]}{[x(i+1/2)-x(i-1/2)][x(i+1)-x(i)][x(i)-x(i-1)]} \tag{71}$$

$$+ \frac{[A_{j+1}-A][z(j)-z(j-1)]-[A_j-A_{j-1}][z(j+1)-z(j)]}{[z(j+1/2)-z(j-1/2)][z(j+1)-z(j)][z(j)-z(j-1)]}$$

and defining

$$\Delta X = [x(i+1/2)-x(i-1/2)][x(i+1)-x(i)][x(i)-x(i-1)] \tag{72}$$

and $$\Delta Z = [z(j+1/2)-z(j-1/2)][z(j+1)-z(j)][z(j)-z(j-1)],$$

$$\nabla^2 A = \{[A_{i+1}-A_i][x(i)-x(i-1)]\Delta Z \tag{73}$$

$$- [A_i-A_{i-1}][x(i+1)-x(i)]\Delta Z + [A_{j+1}-A_j][z(j)-z(j-1)]\Delta X$$

$$- [A_j-A_{j-1}][z(j+1)-z(j)]\Delta X\}/\Delta X\Delta Z.$$

Factoring A_i from (73), it follows that

$$\nabla^2 A \simeq (-A_i\{[\cancel{x(i)}-x(i-1)+x(i+1)-\cancel{x(i)}]\Delta Z \tag{74}$$

$$+ [\cancel{z(j)}-z(j-1)+z(j+1)-\cancel{z(j)}]\Delta X\}$$

$$+ A_{i+1}[x(i)-x(i-1)]\Delta Z + A_{i-1}[x(i+1)-x(i)]\Delta Z$$

$$+ A_{j+1}[z(j)-z(j-1)]\Delta X + A_{j-1}[z(j+1)-z(j)]\Delta X)/\Delta X\Delta Z.$$

Defining

$$\overline{A} = \frac{1}{[x(i+1)-x(i-1)]\Delta Z+[z(j+1)-z(j-1)]\Delta X}[A_{i+1}[x(i)-x(i-1)]\Delta Z \tag{75}$$

$$+A_{i-1}[x(i+1)-x(i)]\Delta Z+A_{j+1}[z(j)-z(j-1)]\Delta X$$

$$+A_{j-1}[z(j+1)-z(j)]\Delta X]$$

and substituting (75) into (74) we have

$$\nabla^2 A \simeq \frac{[(x(i+1)-x(i-1))\Delta Z+(z(j+1)-z(j-1))\Delta X]}{\Delta X \Delta Z} [\bar{A}-A] \cdot \qquad (76)$$

If the grid intervals in the x and z directions are identical, (76) reduces to

$$\nabla^2 A \simeq \frac{4}{(\Delta S)^2} [\bar{A}-A] , \qquad (77)$$

which is the standard approximation for $\nabla^2 A$ for equal grid intervals given in most texts on relaxation techniques.

Substituting (76) into (69)

$$\nabla^2 A \simeq \frac{[(x(i+1)-x(i-1))\Delta Z+(z(j+1)-z(j-1))\Delta X]}{\Delta X \Delta Z} [\bar{A}-A] \simeq F(x,z,t), \qquad (78)$$

or

$$0 = \bar{A}-A - \frac{\Delta X \Delta Z \; F(x,z,t)}{[x(i+1)-x(i-1)]\Delta Z+[z(j+1)-z(j-1)]\Delta X} \cdot \qquad (79)$$

The method of sequential relaxation proceeds as follows. A quess for A is made at an interior grid point. Expression (79) is evaluated. If A is not the proper value

$$RES = \bar{A}-A - \frac{\Delta X \Delta Z \; F(x,z,t)}{[x(i+1)-x(i-1)]\Delta Z+[z(j+1)-z(j-1)]\Delta X} . \qquad (80)$$

In order to eliminate the residual RES, it is added to the quessed value of A. Thus,

$$0 = \bar{A}-A_{NEW} - \frac{\Delta X \Delta Z \; F(x,z,t)}{[x(i+1)-x(i-1)]\Delta Z+[z(j+1)-z(j-1)]\Delta X} \qquad (81)$$

and

$$A_{NEW} = A_{OLD} + \alpha \; RES ,$$

where α is an overrelaxation constant. It was found that

$$\alpha = 1.6 \qquad (82)$$

gave most rapid convergence. Convergence was defined when

$$|RES|_{maximum} \leq .001. \qquad (83)$$

For a problem with only one interior grid point only one relaxation

(with $\alpha = 1$) would be necessary. However, with more interior grid points the change of A by a residual at a grid point affects the values of A at surrounding grid points. Subsequently, the relaxation must be repeated at all interior grid points until the residuals at <u>all</u> interior grid points are arbitrarily small. The method of sequential relaxation requires that new values of A be immediately substituted into the expression for $\overline{A}$ at the next grid point evaluated. Therefore, $\overline{A}$ consists of old and new values of A. For a more complete explanation of sequential relaxation, the reader is referred to Thompson (1961).

In order to solve (81), the values of A or its derivatives at the boundary must be known.

In (64) and (67) certain terms can be defined outside the assumed grid. In these cases the following forms are assumed:

1. For $j = 2$

$$\tilde{w}\frac{\partial\tilde{w}}{\partial z} \simeq \tilde{w}_{j-1}\ \frac{\tilde{w}_{j-1}-\tilde{w}_{j-2}}{z(j-1)-z(j-2)} \simeq \tilde{w}_2\ \frac{\tilde{w}_2}{z(2)} \cdot$$

2. For $j = H - 1$ where H is the top grid point of the model

$$\tilde{w}\frac{\partial\tilde{w}}{\partial z} \simeq \tilde{w}_{H-1}\ \frac{\tilde{w}_H-\tilde{w}_{H-1}}{z(H)-z(H-1)} \cdot$$

3. For $j = 2$

$$\frac{1}{\hat{\Theta}} \simeq \frac{1}{\overline{\Theta}^{j-1/2}} = \frac{1}{\left(\hat{\Theta}_{j-1/2}+\hat{\Theta}_{-3/2}\right)/2} \simeq \frac{1}{\left(\hat{\Theta}_{2+1/2}+\hat{\Theta}_{1+1/2}\right)/2} \cdot$$

4. For $i = N - 1$ where N is the end grid point

$$(\hat{U}+\tilde{U})\frac{\partial\tilde{U}}{\partial x} \simeq (\tilde{U}_{i+1}+\hat{U}_{i+1})\frac{\tilde{U}_{i+2}-\tilde{U}_{i+1}}{x(i+2)-x(i+1)} \simeq 0 \cdot$$

5. For $i = 2$

$$(\hat{U}+\tilde{U})\frac{\partial\tilde{U}}{\partial x} \simeq (\tilde{U}_{i-1}+\hat{U}_{i-1})\frac{\tilde{U}_{i-1}-\tilde{U}_{i-2}}{x(i-1)-x(i-2)} \simeq 0 \cdot$$

In order to satisfy linear computational stability the inequality

$$\Delta t \leq \frac{\Delta x}{U+\sqrt{gH}} \quad \text{must be satisfied.} \tag{84}$$

6. RESULTS

The models have 13 vertical and 21 horizontal grid points defined as

$$\begin{aligned} Z(J) &= 0 && J = 1 \\ Z(J) &= Z(J-1)+300\text{m} && 2 \leq J \leq 11 \\ Z(J) &= Z(J-1)+600\text{m} && 12 \leq J \leq 13 \end{aligned} \tag{85}$$

and

$$\begin{aligned} X(1) &= 0 \\ X(2) &= 20\Delta x \\ X(3) &= 10\Delta x + X(2) \\ X(4) &= 5\Delta x + X(3) \\ X(5) &= 2.5\Delta x + X(4) \\ X(6) &= \Delta x + X(5) \\ &\vdots \\ X(17) &= \Delta x + X(16) \\ X(18) &= 2.5\Delta x + X(17) \\ X(19) &= 5\Delta x + X(18) \\ X(20) &= 10\Delta x + X(19) \\ X(21) &= 20\Delta x + X(20) \,. \end{aligned} \tag{86}$$

The horizontal grid interval is Δx. Heat is introduced into the model by

$$\tilde{\theta} = A \sin \frac{3.14159t}{T} \qquad \begin{matrix} 1 \leq J \leq 2 \\ 7 \leq I \leq 15 \end{matrix}, \tag{87}$$

where T is defined as

$$T = 3600 \text{ sec} \left(\frac{\Delta x}{1 \text{ km}}\right). \tag{88}$$

The large scale velocity and thermal stratification are defined as

$$\hat{U} = 1 \text{ m/sec} ; \tag{89}$$

$$\frac{\Delta\hat{\Theta}}{\Delta z} = B \frac{1°C}{300m} , \qquad 1 \leq J \leq 10 , \tag{90}$$

$$\frac{\Delta\hat{\Theta}}{\Delta z} = \frac{6°}{450m} \qquad \text{(level 10 to 11)} ,$$

$$\frac{\Delta\hat{\Theta}}{\Delta z} = \frac{6°}{300m} \qquad \text{(level 11 to 12)} ,$$

$$\frac{\Delta\hat{\Theta}}{\Delta z} = \frac{12°}{300m} \qquad \text{(level 12 to 13)} .$$

Both models were compared for the values of A, B and ΔX given in table 1. These values were chosen to approximate conditions used in most models of mesoscale atmospheric phenomena.

In order to compare the models, values of the predicted variables were printed after 800 time steps. This corresponded roughly to the time of maximum heating. The time step was determined from

$$\Delta t = .5 \, \Delta x / (\mathcal{U} + \sqrt{gH}) \tag{91}$$

where

$$\mathcal{U} = |\tilde{U} + \hat{U}|_{max} . \tag{92}$$

The velocity $\mathcal{U}$ is the maximum calculated total velocity. Therefore, a shorter time in one model compared to the other for the same A, B and Δx implies a larger maximum total velocity.

The maximum absolute values of the nonhydrostatic component of pressure R, calculated in the first 800 time steps from the anelastic model, are plotted in figure 2 as a function of Δx.

Table 1.

ΔX (km)	$\frac{\Delta X}{\Delta Z}$	A = 5 B = 2	A = 10 B = 2	A = 5 B = 1	A = 10 B = 1	A = 10 B = .5
10	33.3	✓	✓		✓	✓
9	30.0				✓	
8	26.7				✓	
7	23.3			✓	✓	
6	20.0				✓	
5	16.7	✓	✓	✓	✓	✓
4	13.3			✓	✓	
3	10.0			✓	✓	
2	6.7	✓	✓	✓	✓	✓
1	3.3	✓	✓	✓	✓	✓
.3	1.	✓	✓	✓	✓	✓

For the same thermal stratification, the absolute value of R is greater with the larger heat input. Clearly the most rapid decrease of $|R|_{max}$ as a function of Δx occurs for small Δx. In addition, the more stably stratified cases have smaller $|R|_{max}$.

The approximate corresponding pressure deviation is determined from

$$\tilde{\Pi} + \hat{\Pi} = C_p\left(\frac{p}{poo}\right)^K \tag{93}$$

or

$$\tilde{\Pi} = C_p\left[\left(\frac{p}{poo}\right)^K - \left(\frac{\hat{p}}{poo}\right)^K\right], \tag{94}$$

where $\hat{\Pi}$ is defined by

$$\hat{\Pi} = C_p\left(\frac{\hat{p}}{poo}\right)^K . \tag{95}$$

Decomposing p into its large scale and perturbation components and solving for $\tilde{p}$ we find

$$\tilde{p} = poo\left[\frac{\tilde{\Pi}}{C_p} + \left(\frac{\hat{p}}{poo}\right)^K\right]^{\frac{1}{K}} - \hat{p}. \tag{96}$$

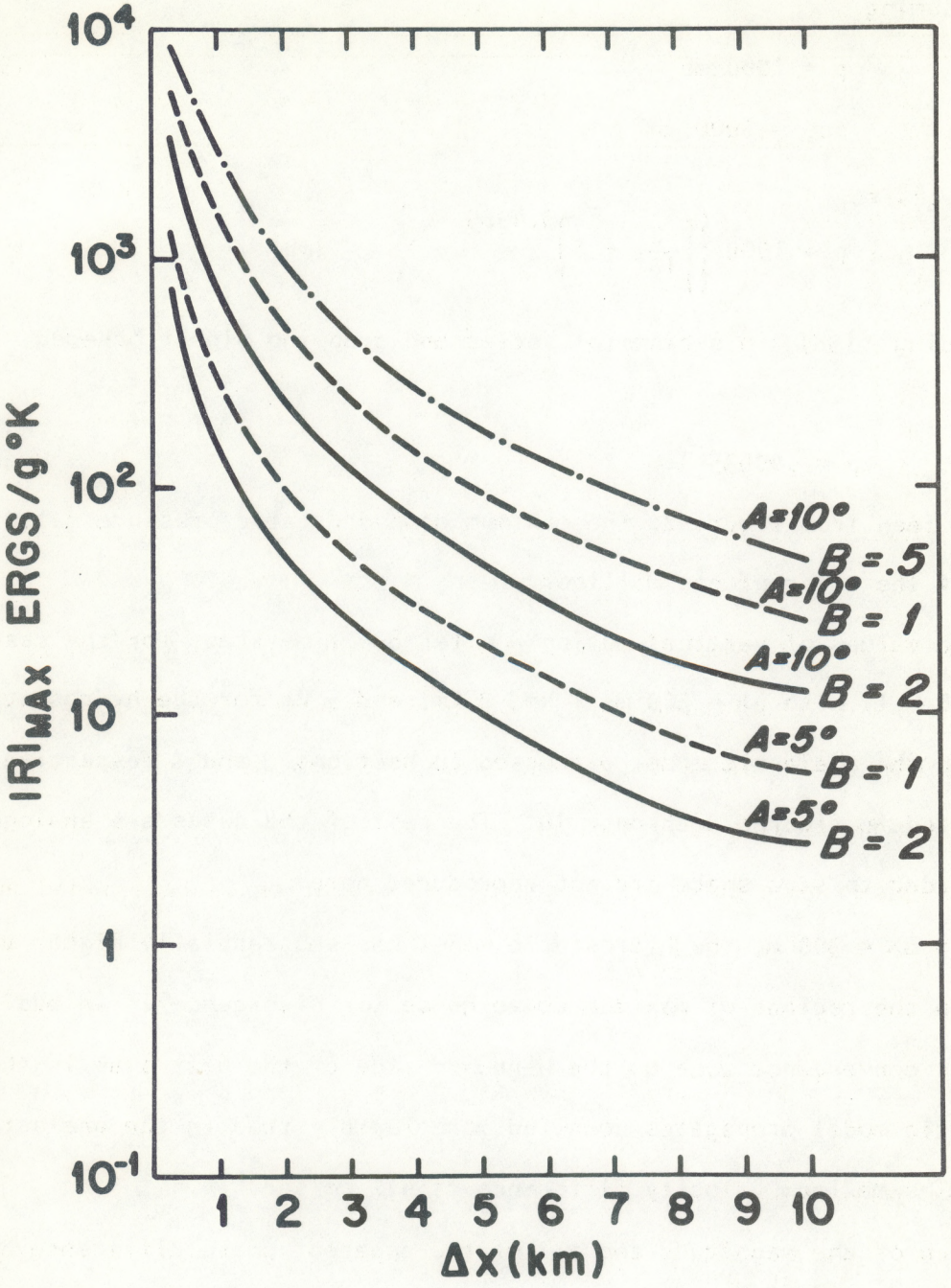

Figure 2. The maximum absolute value of the nonhydrostatic pressure R as a function of horizontal grid interval.

Assuming

$$\hat{p} = 1000 \text{ mb} \tag{97}$$

$$poo = 1000 \text{ mb}$$

(96) reduces to

$$\tilde{p} = 1000 \left\{ \left[\frac{\tilde{\Pi}}{10^7} + 1 \right]^{3.4965} - 1 \right\} . \quad \text{(mb)} \tag{98}$$

or expanding (98) in a binomial series and dropping higher ordered terms,

$$\tilde{p} \simeq .00035 \, \tilde{\Pi}. \tag{99}$$

As seen from figure 2, the maximum nonhydrostatic pressure calculated is of the order of one millibar.

The values of vertical motion $\tilde{w}$ after 800 time steps for the case (A = 5, B = 1) with Δx = 300 m, 1 km, 2 km, and 5 km for the hydrostatic model and the anelastic model discussed in sections 3 and 4 respectively are plotted in figures 3 through 10. The rest of the cases are analogous and in order to save space are not reproduced here.

For Δx = 300 m, the hydrostatic model has substantially higher values of $|\tilde{w}|$ in the regions of maximum convergence (or divergence). In addition, the convergence zone on the windward side of the heat slab in the hydrostatic model propagates downwind more rapidly than in the anelastic model. The maximum velocity difference is 412 cm/sec.

Much of the magnitude and all of the apparent phase difference have disappeared for Δx = 1 km. The maximum velocity difference is 16 cm/sec. Qualitatively, the solutions appear similar; however, the differences may be significant, particularly in a numerical model in which moist thermodynamics are considered.

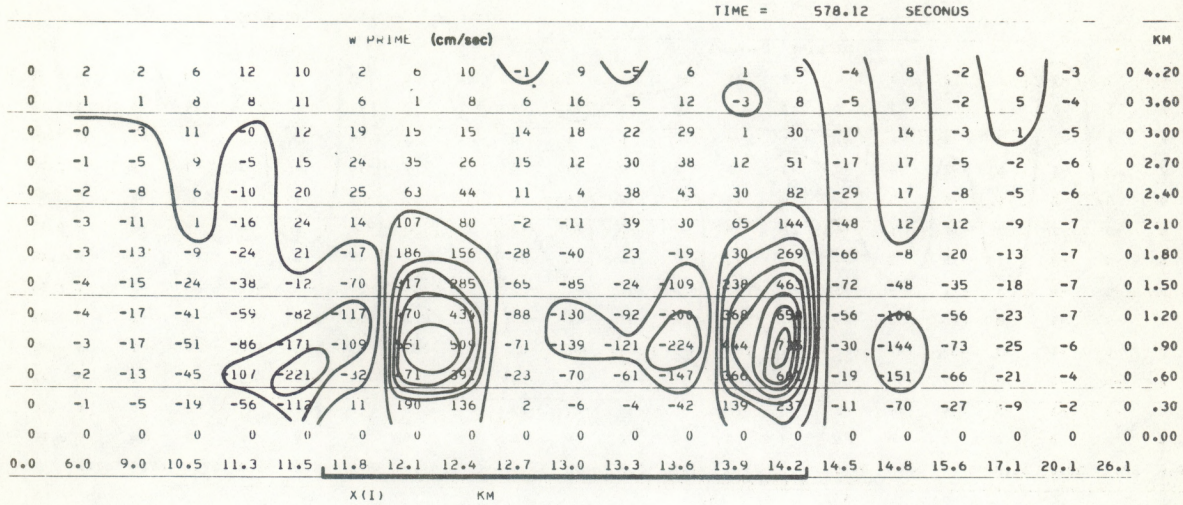

Figure 3. The vertical velocity in the anelastic model: Δx = .3 km, A = 5, B = 1.

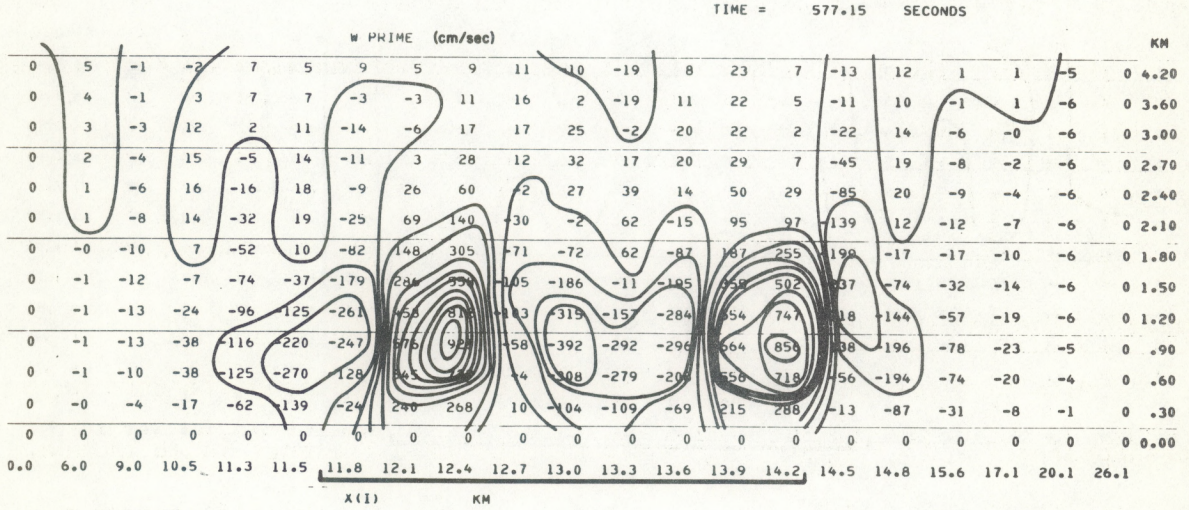

Figure 4. The vertical velocity in the hydrostatic model: Δx = .3 km, A = 5, B = 1.

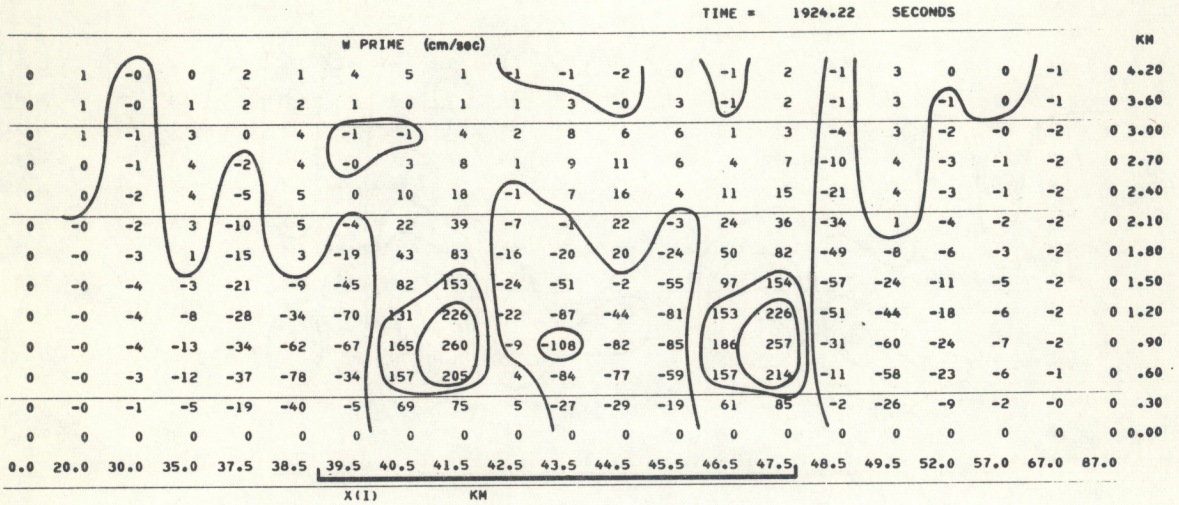

Figure 5. The vertical velocity in the anelastic model: Δx = 1 km, A = 5, B = 1.

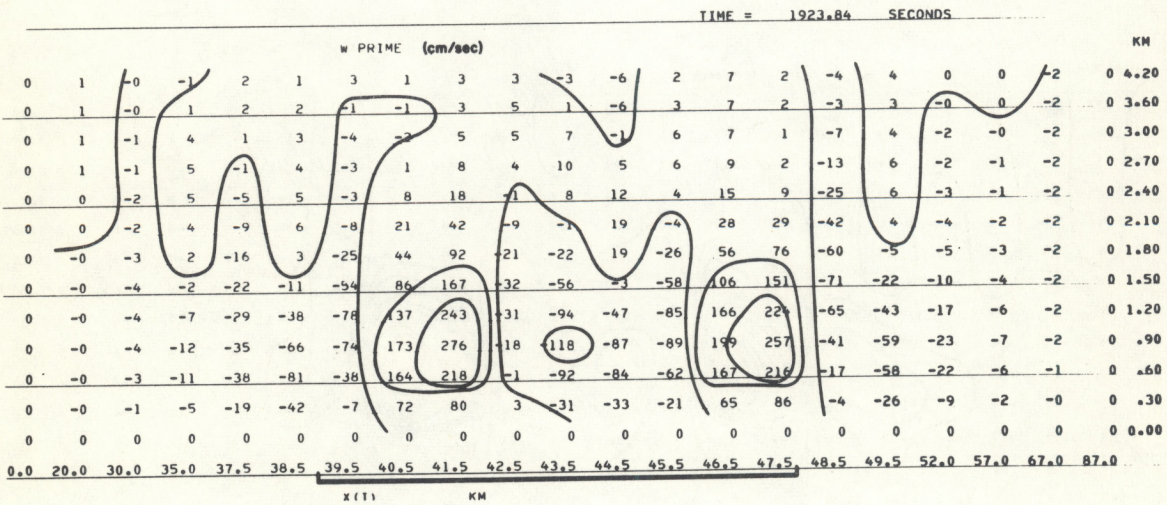

Figure 6. The vertical velocity in the hydrostatic model: Δx = 1 km, A = 5, B = 1.

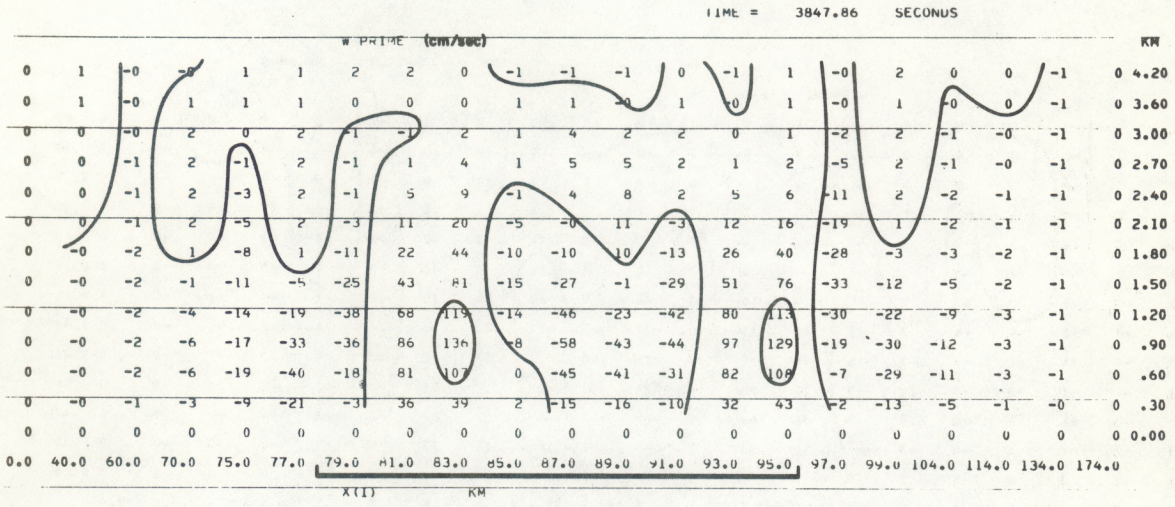

Figure 7. The vertical velocity in the anelastic model: Δx = 2 km, A = 5, B = 1.

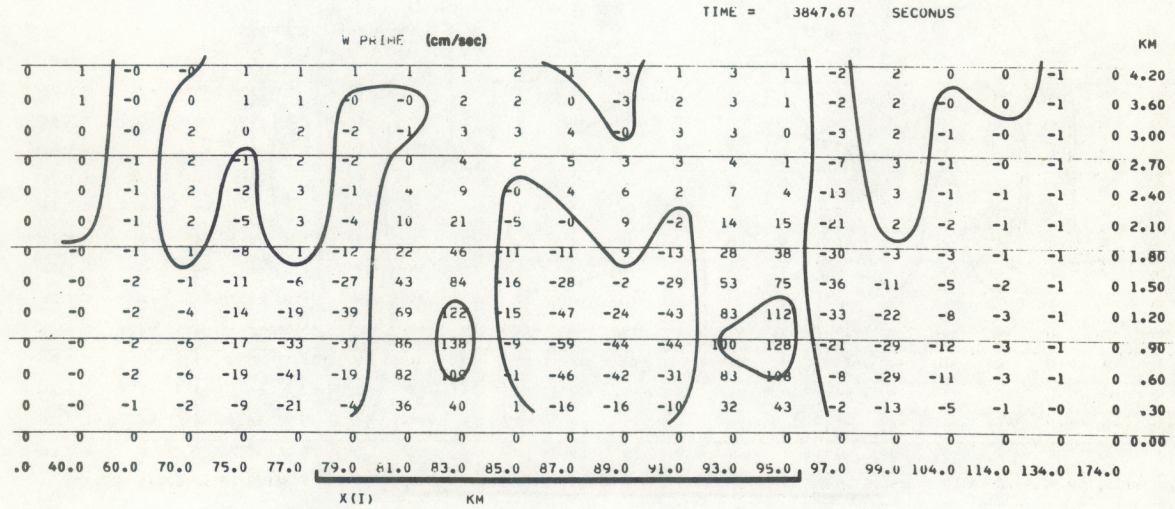

Figure 8. The vertical velocity in the hydrostatic model: Δx = 2 km, A = 5, B = 1.

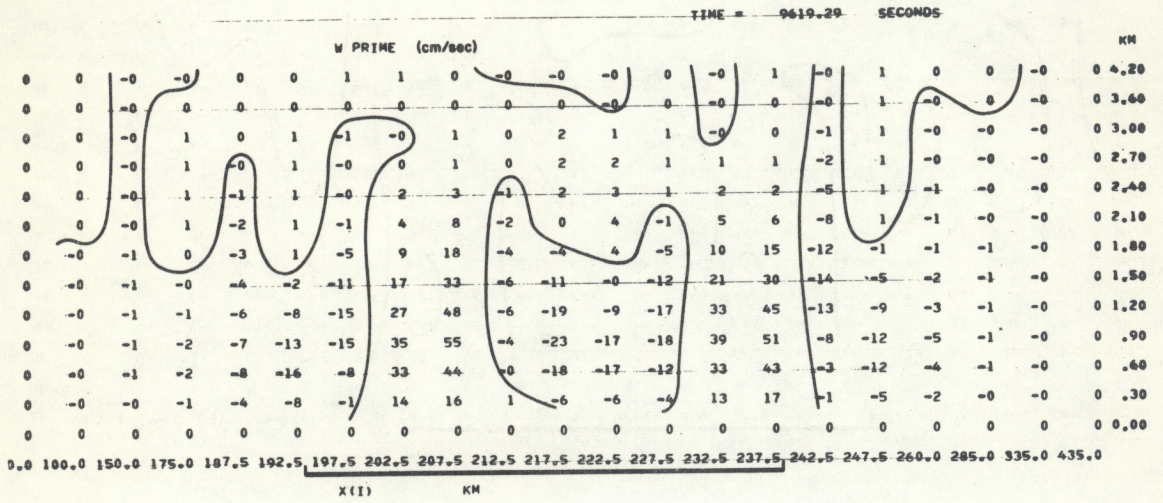

Figure 9. The vertical velocity in the anelastic model: Δx = 5 km, A = 5, B = 1.

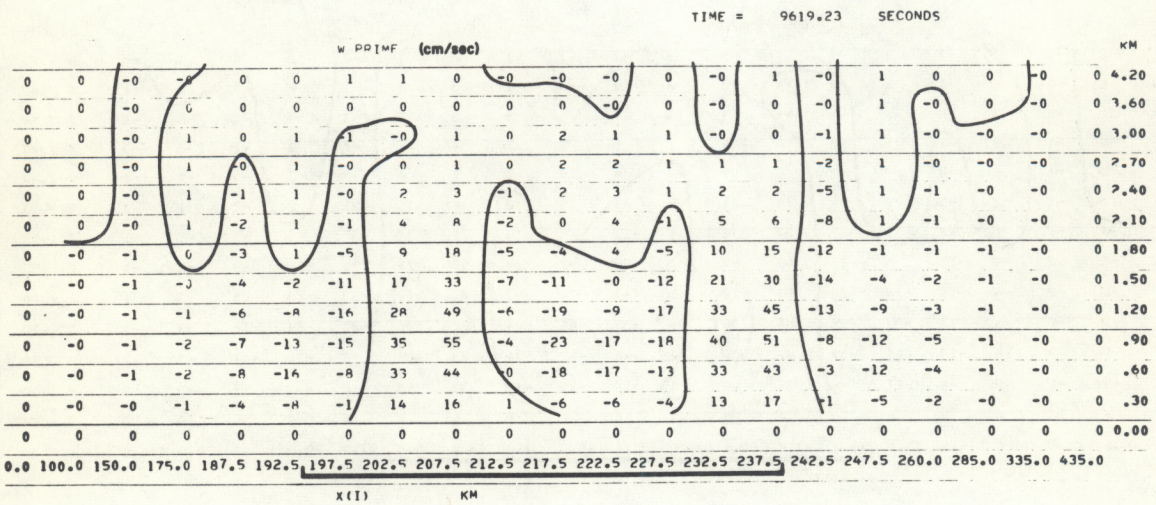

Figure 10. The vertical velocity in the hydrostatic model: Δx = 5 km, A = 5, B = 1.

The solutions converge rapidly as Δx is increased further. At ΔX = 2 km the maximum difference between the two models is only 2 cm/sec.

The maximum absolute values of the vertical velocities and their maximum differences at a grid point at the 800th time step are tabulated in Table 2 for both models. The maximum differences are not necessarily at the same point as the maximum absolute velocities.

The model results are significantly different for Δx = 300 m. Even for the most stable case (A = 5, B = 2) the difference is over 1 m/sec. For the most unstable case (A = 10, B = 5) the difference is 25 m/sec! For all cases with Δx = 300 m the hydrostatic model has the larger maximum absolute velocities. In addition, the windward convergence zone of the hydrostatic model propagates downwind more rapidly than the anelastic model. This accounts for part of the difference in velocities at a grid point between the two models. The increase of heat input for the same stratification increases the difference between the results.

As Δx is increased to 1 km, the solutions are more similar. Only the most unstable case had a difference in velocities greater than 1 m/sec. The differences in the other cases, however, may be significant patticularly in a numerical model which incorporates moist thermodynamics. There is no apparent phase difference in the propagation of the convergence zones between the models.

For larger Δx the differences become progressively smaller. A numerical modeler must ascertain for his individual case whether the differences are significant.

The ratios of the maximum velocity difference and the maximum

Table 2.*

	A = 5 B = 2			A = 10 B = 2			A = 5 B = 1			A = 10 B = 1			A = 10 B = .5		
Δx(Km)	H	N	$\frac{D}{H}$ $\frac{D}{N}$ D	H	N	$\frac{D}{H}$ $\frac{D}{N}$ D	H	N	$\frac{D}{H}$ $\frac{D}{N}$ D	H	N	$\frac{D}{H}$ $\frac{D}{N}$ D	H	N	$\frac{D}{H}$ $\frac{D}{N}$ D
10	12	12	0. 0. 0	41	41	0. 0. 0				90	90	.011 .011 1	132	132	.008 .008 1
9										100	100	.010 .010 1			
8										113	113	.009 .009 1			
7										129	129	.008 .008 1			
6										151	151	.007 .007 1			
5	23	23	.043 .043 1	83	82	.012 .012 1	55	55	.018 .018 1	181	181	.006 .006 1	264	267	.015 .015 4
4							69	69	.029 .029 2	225	226	.009 .009 2			
3							92	91	.022 .022 2	301	303	.020 .020 6			
2	58	58	.034 .034 2	206	206	.019 .019 4	138	136	.022 .022 33	451	454	.038 .037 17	661	687	.068 .066 45
1	116	117	.069 .068 8	413	407	.056 .057 23	276	260	.062 .065 17	902	903	.092 .092 83	1321	1382	.150 .143 198
.3	388	371	.296 .310 115	1376	1331	.379 .392 522	921	735	.447 .561 412	3005	2300	.732 .957 2201	4404	2219	.588 1.166 2588

$H = |\tilde{W}_H|_{max}$ $N = |\tilde{W}_A|_{max}$ $D = |\tilde{W}_H - \tilde{W}_A|_{max}$

*Comparison of the maximum absolute vertical velocities, maximum absolute difference in vertical velocities, and their ratios in the hydrostatic and anelastic models.

absolute velocity for the two models are included in table 2. For Δx = 300 m the percentages range between 25 percent for the most stable case to over 100 percent for the most unstable case. For Δx = 1 km and larger, the percentages are less than 15 percent. Of course, in a nonlinear model, small differences can be important. Nevertheless, there is some support to the adequacy of the hydrostatic model for horizontal to vertical scale ratios as small as 3, as long as heat is introduced into a model over a number of grid points.

The values of the nonhydrostatic component of pressure R and the total pressure $\tilde{\Pi}_A$ at the 800th time step for the case (A = 5, B = 1) are plotted in figures 11 through 18. The maximum absolute value of R occurs

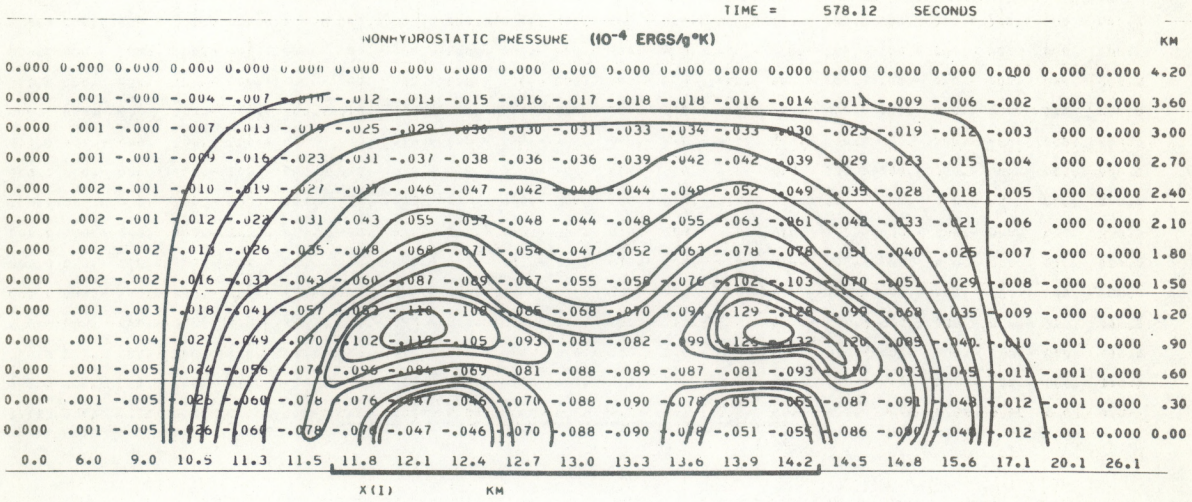

Figure 11. The nonhydrostatic component of pressure R: $\Delta x = .3km$, $A = 5$, $B = 1$.

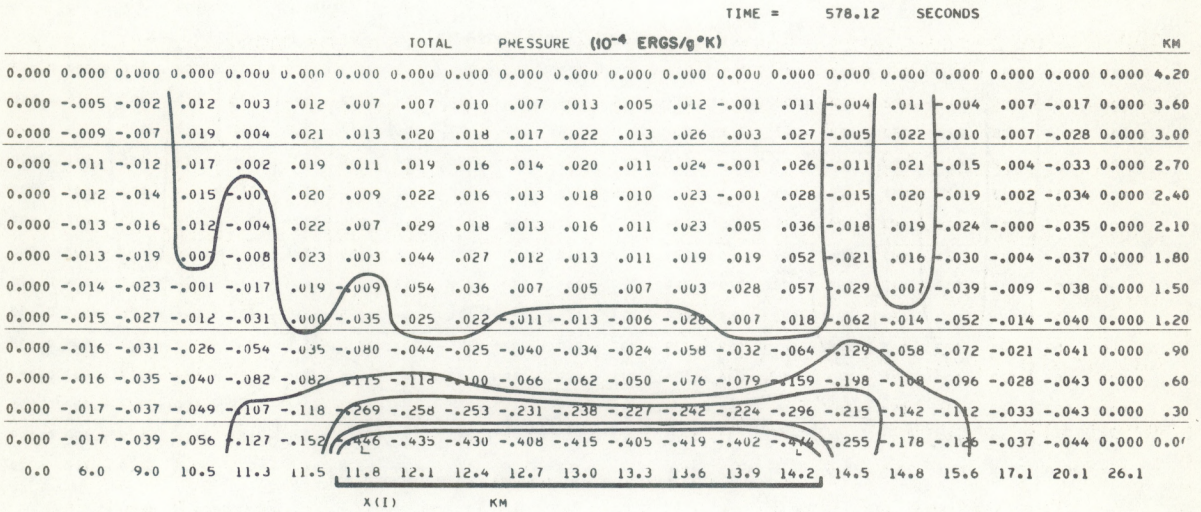

Figure 12. The total pressure $\tilde{\Pi}_A$: $\Delta x = .3km$, $A = 5$, $B = 1$.

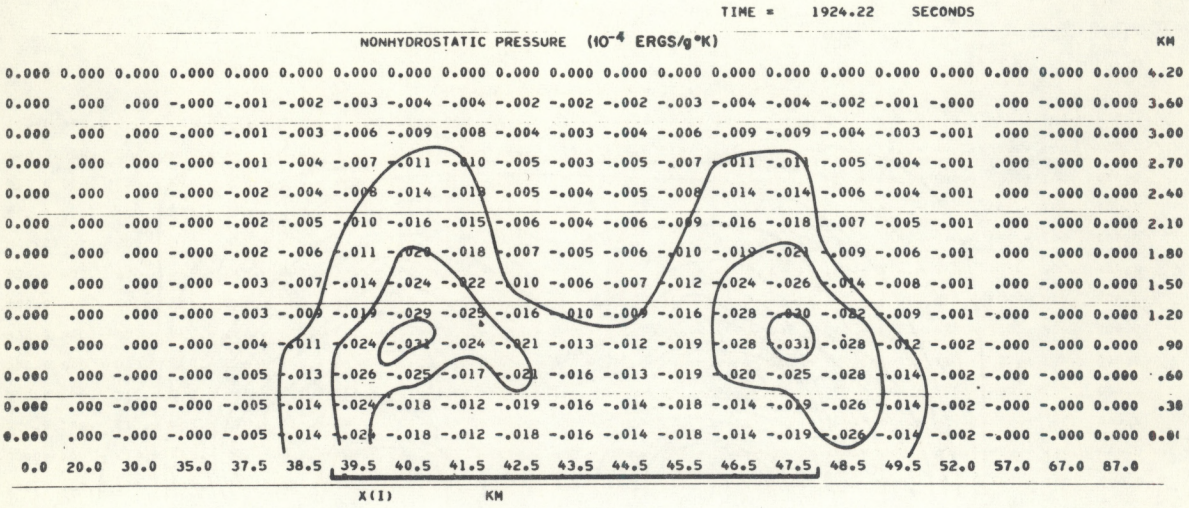

Figure 13. The nonhydrostatic component of pressure R: Δx = 1km, A = 5, B = 1.

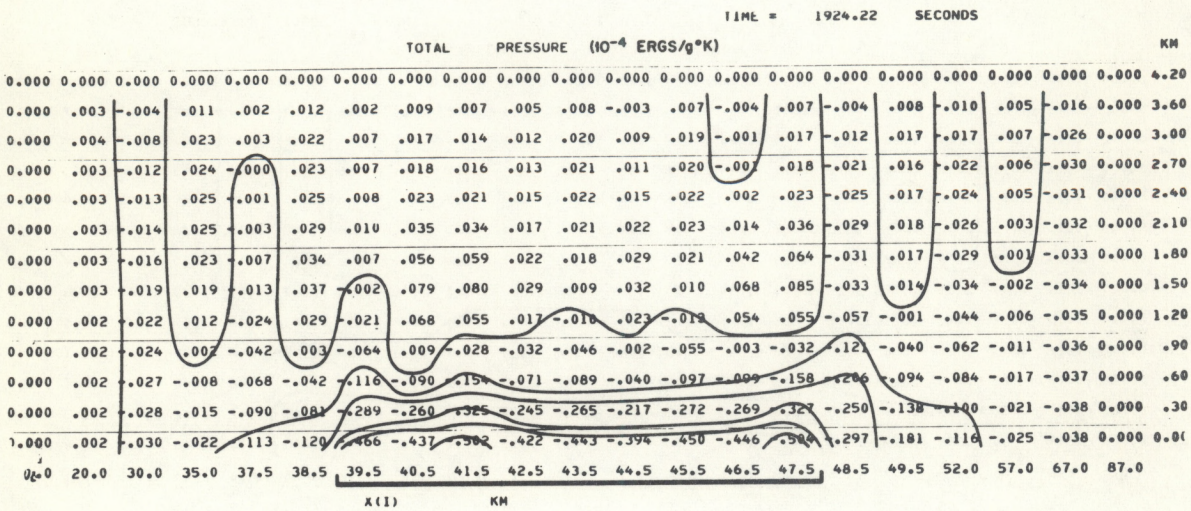

Figure 14. The total pressure $\tilde{\Pi}_A$: Δx = 1km, A = 5, B = 1.

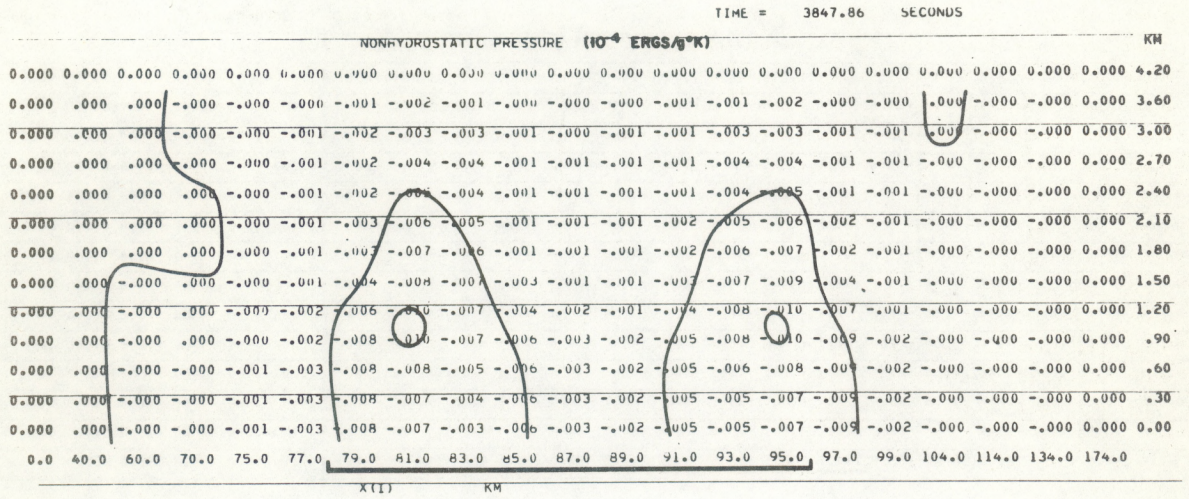

Figure 15. The nonhydrostatic component of pressure R: Δx = 2km, A = 5, B = 1.

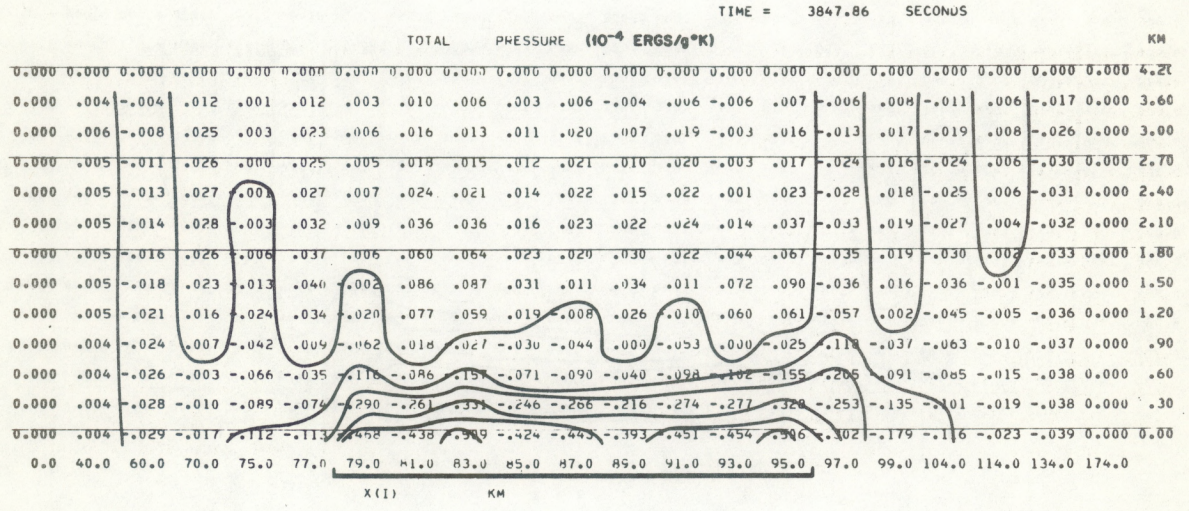

Figure 16. The total pressure $\tilde{\Pi}_A$: Δx = 2km, A = 5, B = 1.

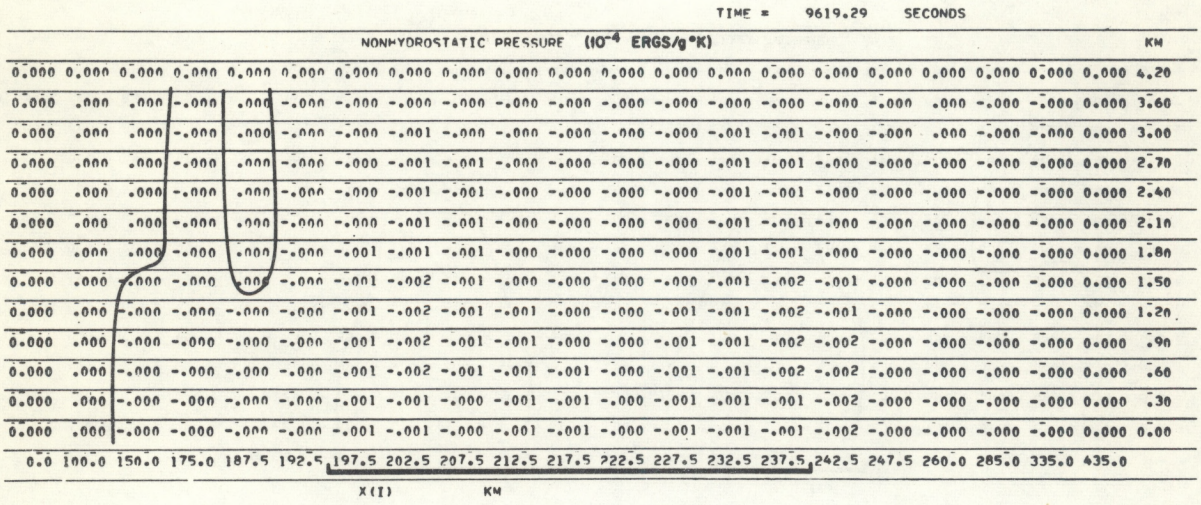

Figure 17. The nonhydrostatic component of pressure R: Δx = 5km, A = 5, B = 1.

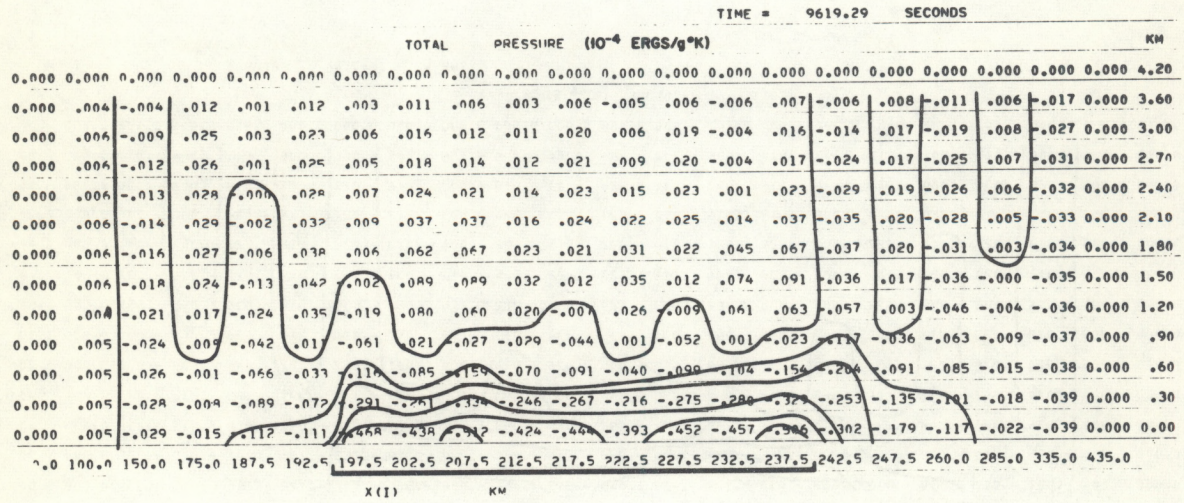

Figure 18. The total pressure $\tilde{\Pi}_A$: Δx = 5km, A = 5, B = 1.

above the maximum convergence zones for all Δx. R approaches zero rapidly as Δx is increased.

In the hydrostatic model, the low level heating creates a low pressure which causes low level convergence. The subsequent vertical motion in a stably stratified atmosphere causes cooling and the generation of a high pressure aloft. The resulting divergence at that level maintains the circulation. The nonhydrostatic pressure gradient is counter to the hydrostatic pressure gradient. The nonhydrostatic pressure creates a relative low pressure aloft and a high pressure near the surface. The result is a smaller amplitude vertical motion field. As Δx is increased, the nonhydrostatic pressure gradient becomes less important. The effect of the nonhydrostatic pressure gradient is sketched schematically in figure 19.

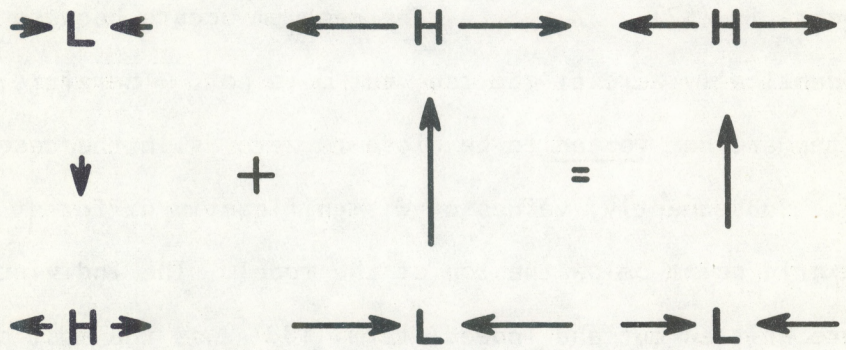

nonhydrostatic pressure		hydrostatic pressure		total pressure
R	+	$\tilde{\Pi}_H$	=	$\tilde{\Pi}_A$

Figure 19.

To verify that the pressure calculated using (64), (65) and (66) corresponds to the pressure calculated using (67), a third model was developed. The equations are identical to the anelastic model already discussed, except that (67) is used to compute the pressure rather than (64), (65) and (66). The elliptic equation for $\tilde{\Pi}_A$ is solved as discussed in section 5.

In order to compare results, the third model was run for the case X = 300 m, A = 5 and B = 1. The values of $\tilde{W}$ calculated from the third model and the anelastic model after 800 time steps are given in figures 20 and 21. Interestingly, the results do not agree. The source of the difference was traced to the term

$$g\frac{\partial}{\partial z}\frac{\tilde{\Theta}}{\hat{\Theta}^2} \simeq \frac{g}{z(j+1/2)-z(j-1/2)}\left[\frac{\tilde{\Theta}_{j+1/2}}{\hat{\Theta}^2_{j+1/2}} - \frac{\tilde{\Theta}_{j-1/2}}{\hat{\Theta}^2_{j-1/2}}\right] \qquad (100)$$

which appears in (67). The problem occurs because $\tilde{\Theta}$ is assumed identically zero at the top, but $\tilde{W}$ is not. Therefore, $\tilde{W}$ values near the top are not <u>forced</u> to be close to zero as in the case of a rigid top. Subsequently, values of $\tilde{\Theta}$ significantly different from zero occur one grid point below the top of the model. The individual terms of (67) were written out and indeed, term (100) was the most significant term near the top. A relative minimum in term (100) occurred in the middle levels of the model.

To further clarify the problem, the anelastic and third model were run without buoyancy effects. Term (100) was neglected in (67) and

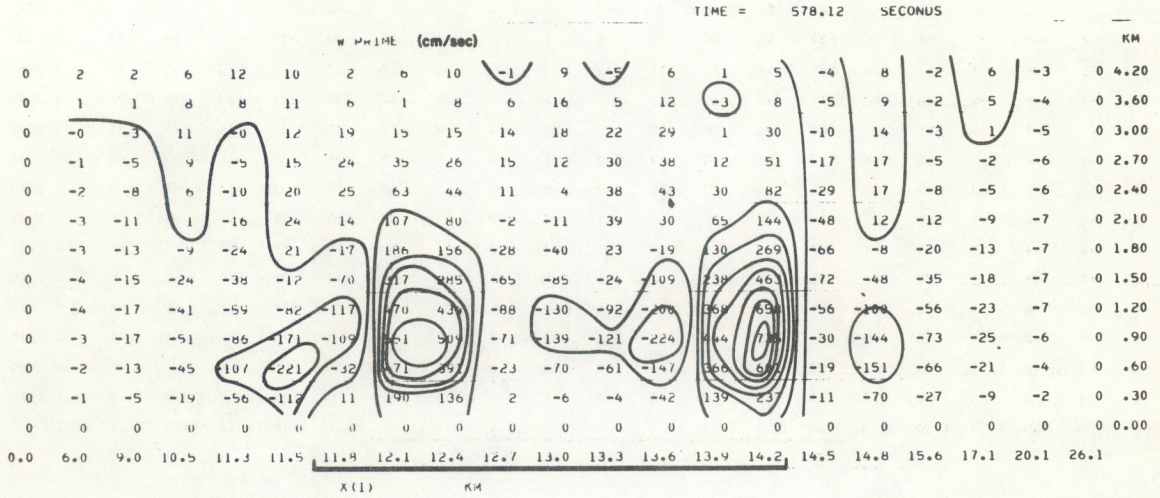

Figure 20. The vertical velocity in the anelastic model: $\Delta x = .3km$, $A = 5$, $B = 1$.

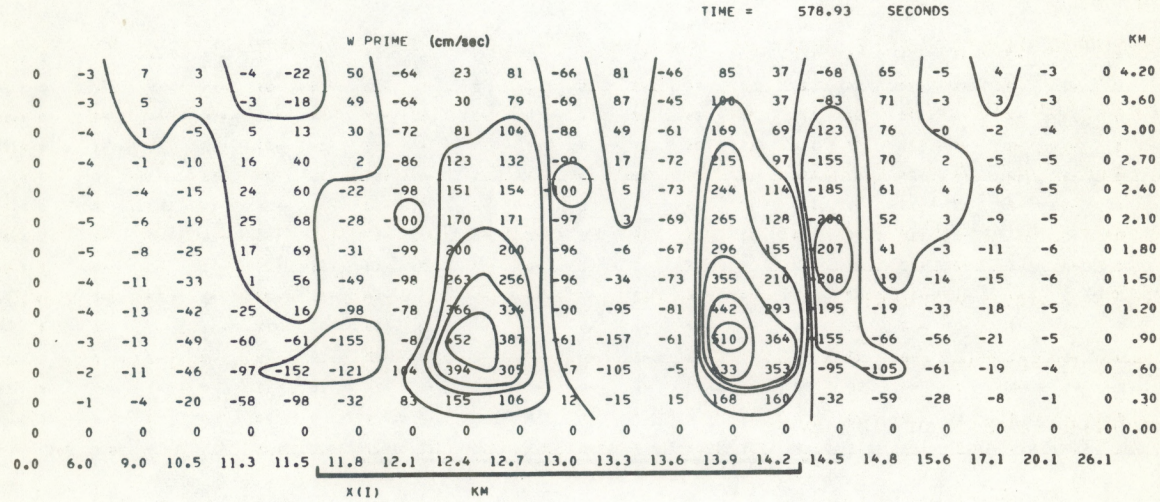

Figure 21. The vertical motion field calculated using (67) to determine pressure: $\Delta x = .3km$, $A = 5$, $B = 1$.

TIME = 589.02 SECONDS

W PRIME (cm/sec) KM

0	-1	-2	-5	-20	95	123	18	26	13	5	1	1	6	-12	-35	-32	-16	-4	-1	0 4.20
0	-1	-2	-5	-20	94	122	18	26	13	5	1	0	5	-12	-35	-32	-16	-4	-1	0 3.60
0	-1	-2	-4	-20	92	119	17	26	12	5	0	-0	5	-12	-35	-31	-15	-4	-1	0 3.00
0	-1	-2	-4	-20	92	118	16	25	12	4	-0	-1	4	-12	-35	-31	-15	-4	-1	0 2.70
0	-1	-2	-4	-20	91	117	15	25	11	3	-1	-1	4	-12	-35	-31	-15	-3	-0	0 2.40
0	-0	-2	-3	-19	91	116	14	23	10	2	-2	-2	3	-13	-35	-30	-14	-3	-0	0 2.10
0	-0	-1	-3	-19	91	114	12	22	8	1	-3	-3	3	-13	-35	-30	-14	-3	-0	0 1.80
0	-0	-1	-2	-17	91	112	9	19	5	-1	-4	-3	2	-14	-35	-29	-13	-3	-0	0 1.50
0	-0	-1	-1	-15	92	109	4	14	2	-3	-5	-4	1	-14	-36	-29	-12	-2	-0	0 1.20
0	-0	-0	-0	-12	92	104	-0	8	-1	-4	-5	-4	1	-16	-37	-27	-11	-2	-0	0 .90
0	-0	-0	0	-8	83	94	-1	2	-1	-2	-2	-2	0	-20	-40	-25	-9	-2	-0	0 .60
0	-0	-0	0	-4	50	58	0	0	-0	-0	-0	-0	-0	-16	-28	-16	-6	-1	-0	0 .30
0	0	0	0	0	0	0	0	0	0	0	0	0	0	0	0	0	0	0	0	0 0.00
0.0	6.0	9.0	10.5	11.3	11.5	11.8	12.1	12.4	12.7	13.0	13.3	13.6	13.9	14.2	14.5	14.8	15.6	17.1	20.1	26.1

X(I) KM

Figure 22. The vertical motion calculated using (64), (65), and (66) to determine pressure with all buoyancy effects neglected: Δx = .3km, $\bar{U}$ = -1m/sec.

TIME = 589.02 SECONDS

W PRIME (cm/sec) KM

0	-1	-2	-5	-21	95	122	18	26	13	5	1	1	6	-11	-34	-31	-16	-4	-1	0 4.20
0	-1	-2	-5	-20	94	121	17	26	13	5	1	0	5	-11	-34	-31	-15	-4	-1	0 3.60
0	-1	-2	-4	-20	92	119	16	25	12	4	0	-0	5	-12	-34	-31	-15	-4	-1	0 3.00
0	-1	-2	-4	-20	91	118	15	25	11	4	-0	-1	4	-12	-34	-31	-15	-4	-1	0 2.70
0	-1	-2	-4	-20	91	116	15	24	11	3	-1	-1	4	-12	-34	-30	-15	-3	-0	0 2.40
0	-0	-2	-3	-19	90	115	13	23	9	2	-2	-2	3	-12	-34	-30	-14	-3	-0	0 2.10
0	-0	-1	-3	-19	90	114	11	21	8	0	-3	-3	3	-13	-35	-30	-14	-3	-0	0 1.80
0	-0	-1	-2	-17	91	112	8	18	5	-1	-4	-3	2	-13	-35	-29	-13	-3	-0	0 1.50
0	-0	-1	-1	-15	92	109	4	14	2	-3	-5	-4	1	-14	-35	-28	-12	-2	-0	0 1.20
0	-0	-0	-0	-12	92	104	-1	7	-1	-4	-5	-4	1	-16	-37	-27	-11	-2	-0	0 .90
0	-0	-0	0	-8	83	94	-1	2	-1	-2	-2	-2	0	-20	-39	-25	-9	-2	-0	0 .60
0	-0	-0	0	-4	50	58	0	0	-0	-0	-0	-0	-0	-16	-28	-16	-6	-1	-0	0 .30
0	0	0	0	0	0	0	0	0	0	0	0	0	0	0	0	0	0	0	0	0 0.00
0.0	6.0	9.0	10.5	11.3	11.5	11.8	12.1	12.4	12.7	13.0	13.3	13.6	13.9	14.2	14.5	14.8	15.6	17.1	20.1	26.1

X(I) KM

Figure 23. The vertical motion calculated using (67) to determine pressure with all buoyancy effects neglected: Δx = .3km, $\bar{U}$ = -1m/sec.

$\tilde{\Pi}_H$ was neglected in (66) and (61). Motion was initiated by an initial velocity perturbation given by

$$\tilde{U} = -1 \text{ m/sec} \qquad \begin{matrix} 1 \leq J \leq 2 \\ 7 \leq I \leq 15. \end{matrix} \tag{101}$$

The results after 800 time steps are given in figures 22 and 23. Despite the obvious inconsistency of the boundary condition at the top and the lack of damping of convergence by the stable stratification, the results are almost identical. Indeed, when the individual function values in

$$\nabla^2 R = F(x,z,t) \tag{102}$$

and

$$\nabla^2 \tilde{\Pi}_A = G(x,z,t)$$

are written out

$$G(x,z,t) \simeq F(x,z,t) \tag{103}$$

at each grid point despite the fact that they are calculated somewhat differently.

The model results using (67) to calculate the pressure were not improved by increasing Δx. The same inconsistency was introduced and rapidly destroyed the similarity with the anelastic model discussed in this paper.

7. SUMMARY AND CONCLUSIONS

The hydrostatic assumption is invalid for $\Delta x = 300$m for all cases investigated in this study. This corresponds to a D/L ratio of order unity. For Δx to ΔZ ratios of three and greater, the hydrostatic assumption may be adequate. The more stable the thermal stratification and the smaller the heat input, the better the approximation is for a given Δx.

Each numerical modeller, however, must ascertain for his particular case if the hydrostatic assumption is satisfactory. Certainly the introduction of moist thermodynamics will complicate the consideration.

The non-hydrostatic pressure gradient is counter to the hydrostatic pressure gradient. For most cases, particularly with $\Delta x = 300m$, the result is a smaller amplitude vertical motion field in the anelastic model as compared to the hydrostatic model. In addition, the propagation of the windward convergence zone is slower in the anelastic model for $\Delta x = 300m$.

A new technique to compute the anelastic pressure has been introduced. This method has the advantage that the effect of buoyancy on the pressure is integrated as in a hydrostatic model rather than being differentiated and included in an elliptic differential equation. In addition, because this term is evaluated separately from the elliptic equation, any errors introduced by inconsistencies in the boundary conditions are minimized rather than propagated through the entire field as is the manner of solving an elliptic differential equation. Also, by decomposing pressure into a hydrostatic and non-hydrostatic component, additional information regarding pressure can be obtained.

Finally, this paper does not represent an exhaustive study of the subject. Variations of number of grid points in which heat is introduced, different vertical grid intervals as well as different synoptic velocities have not been examined. However, the author feels the results improve our quantitative understanding of the adequacy of the hydrostatic asuumption for various grid intervals as long as heat is introduced over a number of grid points. Individual modellers must judge the applicability of these results to their models.

8. ACKNOWLEDGMENTS

The author appreciatively acknowledges the useful advice and stimulating discussions with Dr. William Cotton of the Experimental Meteorology Laboratory.

The author would also like to thank other members of EML, particularly Dr. Joanne Simpson for the opportunity to do the experiments, Mrs. Constance A. Arnhols who painstakingly typed the manuscript, and Mr. Robert Powell who did an excellent job drafting the figures.

REFERENCES

Brundidge, K.C., K.G. Cottrell, D. Djuric, R.A. Perry and R.T. Song (1971), Project Themis, Prediction of Environmental Parameters, Annual Report, Vol. 1, Final Report Subtask A, Numerical Simulation of Convection, ECOM-0073-5, 193 pp.

Delage, Y. and P.A. Taylor (1970), Numerical studies of heat island circulations, Boundary Layer Meteorology 1, 201-226.

Dutton, J.A. and G.H. Fichtl (1969), Approximate equations of motion for gases and liquids, J. Atmos. Sci. 26, 241-254.

Estoque, M. (1961), A theoretical investigation of the sea breeze, Q. J. Roy. Met. Soc. 87, 136-146.

_____, (1962), The sea breeze as a function of the prevailing synoptic stiuation, J. Atmos. Sci. 19, 244-250.

Estoque, M. and C. Bhumralkar (1968), Theoretical studies of the atmospheric boundary layer, June 1968, Final Report: ECOM-6762-F, 43 pp.

Haltiner, G.J. (1968), Numerical Weather Prediction, Navy Weather Research Facility, 88 pp.

Hide, R. (1958), An experimental study of thermal convection in a rotating fluid, Phil. Trans. Roy. Soc. London 250, 441-478. Cited by Hovermale (1965).

Hovermale, J. (1965), A nonlinear treatment of the problem of airflow over mountains, Ph.D. Dissertation, Pennsylvania State University, 88 pp.

Lumley, J.L. and H.A. Panofsky (1966), The structure of atmospheric turbulence, Interscience Publishers, 239 pp.

McPherson, R.D. (1970), A numerical study of the effect of a coastal irregularity on the sea breeze, J. Appl. Meteor. 9, 767-777.

Molenkamp, C.R. (1968), Accuracy of finite difference methods applied to the advection equation, J. Appl. Meteor 7, 160-167

Moroz, W.J. (1967), A lake breeze on the eastern shore of Lake Michigan: observations and model, J. Atmos. Sci. 24, 337-355.

Neumann, J. and Y. Mahyer (1971), A theoretical study of the land and sea breeze circulation, J. Atmos. Sci. 28, 532-542.

Ogura, Y. (1963), The evolution of a moist convective element in a shallow, conditionally unstable atmosphere: a numerical experiment, J. Atmos. Sci. 20, 407-424. Cited by Rosenthal (1969).

Ogura, Y. and J. Charney (1961), A numerical model of thermal convection in the atmosphere, Proc. Int. Symp. Num. Wea. Pred., Tokyo, Japan. Nov. 7-13, 1960, 431-450.

Orville, H.D. (1964), On mountain upslope winds, J. Atmos. Sci. 21, 622-633. Cited by Rosenthal (1969).

Rosenthal, S. (1969), Experiments with a numerical model of tropical cyclone development. Some effects of radial resolution, Tech. Memo. ERLTM-NHRL87, 47 pp.

Richtymer, R.D. (1962), A survey of difference methods for non-steady fluid dymamics, NCAR Tech. Notes 63-67, 25 pp. Cited by Rosenthal (1969).

APPENDIX

List of Symbols

U_i	velocity
U	horizontal velocity
W	vertical velocity
X_i	space coordinate
t	time
X	horizontal coordinate
Z	vertical coordinate
ρ	density
g	gravity
Ω_j	rotation
Θ	potential temperature
Π	$c_p \left(\frac{p}{poo}\right)^{\kappa}$ (scaled pressure)
H	depth of model
c_p	specific heat at constant pressure
poo	reference state pressure
κ	$R_d/c_p \simeq .286$
R_d	gas constant for dry air
Π_H	hydrostatic pressure
Π_A	total pressure: hydrostatic pressure plus nonhydrostatic pressure
$K^{(m)}_{ij}$	eddy exchange coefficient for momentum
$K^{(m)}_{j}$	eddy exchange coefficient for heat
$A^{(x)}$	temperature amplitude
T	half period of temperature oscillation
R	nonhydrostatic component of pressure

Note on tensor notation

1. Repeated indices are summed over the indicated range. A line under an index indicates that index is not summed over.

2. Single indices are not summed over. They assume the values indicated.

Finite difference notation

$$\tilde{U} \equiv \tilde{U}^{\tau}_{i,j}$$

$$\tilde{W} \equiv \tilde{W}^{\tau}_{i,j}$$

$$\tilde{\Pi} \equiv \tilde{\Pi}^{\tau}_{i,j}$$

$$\tilde{\Theta} \equiv \tilde{\Theta}^{\tau}_{i,j+1/2}$$

$$\hat{\Theta} \equiv \hat{\Theta}_{j+1/2}$$

USCOMM - ERL